In presenting this thesis in partial fulfillment of the requirements for an advanced degree at Idaho State University, I agree that the library shall make it freely available for inspection. I further state that permission for extensive copying of my thesis for scholarly purposes may be granted by the Dean of Graduate Studies, Dean of my academic division, or by the University Librarian. It is understood that any copying or publication of this thesis for financial gain shall not be allowed without my written permission.

Signature_____

Date_____

The Use of Remote Sensing Indices to Determine Wildland Burn Severity In Semiarid Sagebrush Steppe Rangelands Using Landsat ETM+ and SPOT 5

by

Jill M. Norton

A thesis submitted in partial fulfillment

of the requirements for the degree of

MASTER OF SCIENCE

IN

GEOGRAPHIC INFORMATION SCIENCES

Department of Geosciences

Idaho State University

2006

To the Graduate Faculty:

The members of the committee appointed to examine the thesis of Jill M. Norton find it satisfactory and recommend that it be accepted.

_____

Dr. Nancy F. Glenn
Major Advisor

_____

Dr. Matthew J. Germino
Committee Member

_____

Dr. Anthony W. Stocks
Graduate Faculty Representative

Acknowledgements

I am indebted to Dr. Nancy Glenn, my major advisor for her insightful guidance, endless help, and benevolent patience throughout my graduate career. I am thankful to Dr. Matt Germino for his frequent edits and guidance in addition to providing accommodation in his supportive lab facility. I am grateful, as well to my other committee members, Tony Stocks and Steve Seefeldt, for believing in me and inspiring self-confidence.

To my family and friends, near and far, thank you for your compassion, love, and support throughout my academic career. I could not have done it without you! Mom, Dad, Paule, April, and James thank you for the tremendous amount of support and love you've given me. Dan, Erik, Jane, Jen, Jesse, John, Monique, Penny, Ru, Sara, Tony, and the many others involved in my graduate experience—thank you so very much!

This project would not have been possible without the funding from the National Aeronautics and Space Administration (NASA) grant #NNG05GB05G. The U.S. Sheep Experiment Station in Dubois, Idaho offered their facilities and friendly support during the field seasons. I thank Bret Taylor and Ada Williamson for helping with and encouraging the success of two field seasons; and I thank Steve Seefeldt for facilitating with the prescribed burn.

Table of Contents

PHOTOCOPY USE AND AUTHORIZATION……..…..i
TITLE PAGE…….....ii
COMMITTEE APPROVAL PAGE…….iii
ACKNOWLEDGEMENTS…….. ...iv
TABLE OF CONTENTS……...…v
LIST OF FIGURES…….....vii
LIST OF TABLES ……....viii
THESIS ABSTRACT……...ix
1.0 Introduction……....1
1.1 Introduction and Statement of the Problem……...1
1.2 Background……..…..…3
1.2.1 Remote Sensing…….…...…3
1.2.2 Remote Sensing of Vegetation in Semi-Arid Environments…...4
1.2.3 Remote Sensing of Burns and Burn Severity…….....6
1.3 Study Area…….....10
2.0 Field Methods……...…11
2.1 Introduction……..11
2.1.1 Pre-Field Operations……...…14
2.1.2 Field-Based Ocular Estimates……14
2.1.3 Field-Based Point Frame Measurements……...15
2.2 Field Methods—Sampling Stages……17
2.2.1 Pre-Fire Sampling……..17
2.2.2 Prescribed Fire……...17
2.2.3 Post-Fire Sampling……18
2.2.4 Post-Field Operations……20
3.0 Remote Sensing Methods……20
3.1 Image Acquisition……20
3.2 Overview of Image Processing……21
3.3 Pre-processing of Imagery……...…24
3.3.1 Radiometric Correction……..24

3.3.2 Geometric Correction…….……25
3.4 Remote Sensing Indices……...26
3.4.1 Single Date Indices……27
3.4.2 Multi-Date Indices.....…….…….……28
4.0 Accuracy Assessment……...……...29
4.1 Relating Remote Sensing Indices to Field Data……..29
4.2 Validation…...…….30
5.0 Results……..31
5.1 Burn Versus Unburned Index Results…...……..31
5.2 Burn Severity Index Results.....32
6.0 Discussions and Conclusions……...……33
REFERENCES……66
APPENDIX I. Results of 10 Remote Sensing Indices…..……...73
APPENDIX II. Other remote sensing indices applied…….…….……..….79
APPENDIX III. Details of the Landsat and SPOT sensors…...…….……83
APPENDIX IV. Assessment of Hypothesis #2: Can burn severity be predicted with fuel load?.....84
APPENDIX V. Research Notes: Comparison of Field Methods…….86
Introduction……..86
Methods……89
Results……..92
Discussions and Conclusions……...……93
References……96
Tables and Figures……...98

LIST OF FIGURES

Figure 1. Location of the Hitching Post pasture study area in Southeastern Idaho……...…….42

Figure 2. A sample effort curve is used to determine the necessary sampling intensity from one 20 x 40 m plot…….....……43

Figure 3. Approximate location of 15 point frames within each 20x40m plot…….....44

Figure 4. Pre- and post-fire sampling plot locations, prescribed fire boundaries, and bulldozer-created fireline……..45

Figure 5. Using pre-fire and post-fire SPOT imagery and (n = 36) homogenous point frame plot reflectance averages, reflectance changes the most in red and near infrared reflectances……46

Figure 6. Using pre-fire and post-fire Landsat imagery and (n=32) homogenous point frame plot reflectance averages, reflectance changes the most in near infrared and shortwave infrared bands…….47

Figure 7. Example of a categorical scatterplot of burn severity classes: the Landsat MSAVI index…….48

Figure 8. The best burn severity index was the RdNBR using Landsat data…..49

Figure 9. Comparison of the burn severity Landsat and SPOT NDSWIR Results……..50

Figure 10. The best burn versus unburned index was the SAVI using SPOT data……...51

Figure 11. Using the pre-fire data set, point frame estimates are fairly correlated with ocular estimates (n = 49) in the same area for shrub and bareground……...99

Figure 12. Using the post-fire data set, the best correlation between point frame estimates and ocular estimates are for shrub (best overall correlation) and forb……..……100

LIST OF TABLES

Table 1. Remote sensing indices that were explored to find the best burn/no burn algorithm and the best burn severity algorithm…….52

Table 2. Categorical groups of percent cover……..……..53

Table 3. Field attributes for all ocular estimates…….…....54

Table 4. Field attributes for all point frame plots ……..…..……55

Table 5. Description of burn severity categories based on an ocular estimate……..….....56

Table 6. Dates and location of SPOT and Landsat imagery……..……57

Table 7. Root Mean Square Error (RMSE) of the Landsat and SPOT data…..58

Table 8. Ratio of the number of training plots to validation plots when assessing all remote sensing indices……..……59

Table 9. The Landsat dNBR burn severity index error matrix table with Kappa results: …….……60

Table 10. ‘Burned versus unburned’ remote sensing index accuracies and kappa statistics using SPOT 5 imagery..……..……61

Table 11. The SPOT SAVI index error matrix table with 100% overall accuracy……...62

Table 12. ‘Burned versus unburned’ remote sensing index accuracies and Kappa statistics using Landsat ETM+ imagery…….....63

Table 13. ‘Burn severity’ remote sensing index accuracies and kappa statistics using SPOT 5 imagery.....……..64

Table 14. ‘Burn severity’ remote sensing index accuracies and kappa statistics using Landsat ETM+ imagery……..……65

Table 15. Results of all SPOT burned versus unburned remote sensing indices…….……..…73

Table 16. Results of all Landsat burned versus unburned remote sensing indices……..74

Table 17. Results of all SPOT burn severity remote sensing indices……..75

Table 18. Results of all Landsat burn severity remote sensing indices……..…..77

Table 19. Other remote sensing indices to detect burn severity……..……80

Table 20. 'Burn severity' accuracies and kappa statistics for other remote sensing indices using SPOT 5 imagery…….……..81

Table 21. 'Burned versus unburned' accuracies and kappa statistics for other remote sensing indices using SPOT 5 and imagery……82

Table 22. Comparison of Landsat 7 and SPOT 5 sensor characteristics…….83

Table 23. Attributes of the ocular and point frame field methods……...98

Table 24. Maximum percent of cover within each cover class using ocular and point frame data collected before the fire.....101

Table 25. Maximum percent of cover within each cover class using ocular and point frame pre-fire data collected after the fire……..……..……101

The Use of Remote Sensing Indices to Determine Wildland Burn Severity In Semiarid Sagebrush Steppe Rangelands Using Landsat ETM+ and SPOT 5

Thesis Abstract—Idaho State University (2006)

This study evaluates ten remote sensing indices to detect burned areas and burn severity in a southeastern Idaho study area. While fire-related studies have been performed in forested ecosystems, few have been conducted in sagebrush steppe rangelands. Burn severity, defined as the completeness of aboveground vegetation removal during the burn, is useful in determining the type and location of treatment(s) that land managers can implement to speed recovery, and thus assess effectiveness and speed of landscape recovery. This study utilizes pre- and post-fire field based sampling as ground control for image processing of Landsat ETM+ and SPOT 5 multispectral imagery. Single and multi-date indices were validated through accuracy assessment techniques. Remote sensing indices comparing burned with unburned areas had better overall, user's, and producer's accuracies than indices comparing levels of burn severity. The best burn versus unburned index was the Soil Adjusted Vegetation Index (SAVI; 100% overall accuracy) derived from SPOT imagery, and the best burn severity index was the relative differenced Normalized Burn Ratio (RdNBR; 73% overall accuracy) derived from Landsat imagery. These two indices provided the highest user's and producer's accuracies.

1.0 Introduction

1.1 Introduction and Statement of the Problem

Roughly 35-40% of the terrestrial earth's surface is comprised of arid and semi-arid lands (Rahman and Gamon, 2004; Anderson and Inouye, 2001; McGwire et al., 2000). Specifically, sagebrush steppe is the largest semiarid vegetation type in North America, yet it is critically endangered (Anderson and Inouye, 2001). In order to properly manage rangelands, it is essential to have a clear understanding of their ecological processes, functions, and the mechanisms driving change. For instance, fire has a powerful influence on ecosystem function and dynamics. Wildland fire is the primary cause of destruction in sagebrush steppe, where erosion hazard is high, vegetation is dry, and perennial vegetation recovery rates are slow (Ruiz-Gallardo et al., 2004; Whitford, 2002; and Wright and Bailey, 1982). Fire frequencies range from 15-100 years in sagebrush steppe ecosystems (Wright and Bailey, 1982; Ratzlaff and Anderson, 1995; Miller and Rose, 1999; Harniss and Murray, 1973; Watts and Wambolt 1996; and Brown et al., 2000). Moreover, fire frequencies have increased due to an abundance of fire-prone introduced annuals (i.e. *Bromus* tectorum) or short-lived perennials, and due to fuel loading following many years of fire suppression (Anderson and Inouye, 2001; Keeley et al., 1999; Diaz-Delgado et al., 2002; Obrist et al., 2003; Whisenant, 1990; Brown et al., 2000). From 1995 to 2005 wildland fires burned approximately 24,277,866 ha in the US compared with 19,828,021 ha burned between 1960 to 1970 (NIFC, 2006). When managing rangelands, the multitude of fire effects need to be accounted for and monitored to update fuel model/vegetation data bases, and to assess ecosystem damage and benefit, the success or failure of a

treatment, the possible need for rehabilitation, and vegetation change effects for wildlife concerns or erosion potential (Lutes et al., 2003). The need for information about burned areas (i.e. perimeter and area) has increased; moreover, it is essential to understand the heterogeneity of burn severity patterns within a fire perimeter (van Wagtendonk et al., 2004). Burn modeling and maps (severity, frequency, pattern, size, etc.) provide useful information for land planning, risk assessment, and evaluation of ecological conditions such as the structure, composition, and function of ecosystems (Morgan et al., 2001). Knowledge of within-burn variability fosters understanding of fire's effects such as burn severity, vegetation recovery, and succession enhancing post-fire rehabilitation and remediation efforts (Roy et al., 2006). For example, burn severity information is useful in determining the type and location of treatment(s) that land managers can implement and later assess effectiveness and rate of landscape recovery. Simple and cost-effective techniques need to be established to map fire effects, such as burn severity and extent, within rangelands. Remote sensing with satellite imagery offers the ability to evaluate burned areas across multi-temporal and multi-spatial scales (Morgan et al., 2001). Satellite data are useful for examining fire effects because 1) they can be used to qualitatively and quantitatively evaluate vegetation over multi-temporal and spatial scales, 2) they can be relatively low in cost, 3) they can systematically cover large and inaccessible areas (in many instances fires are located in remote areas), and 4) they can capture data from parts of the electromagnetic spectrum that humans cannot sense (i.e. infrared), which provide useful information specific to vegetation and soils.

Definitions of burn severity differ, as well as the amount of time elapsed between a fire occurrence and when burn severity is assessed (Ryan and Noste, 1983; Miller and Yool, 2002; Roy et al., 2006; Key and Benson, 2006); however, for this research, burn severity is defined as the completeness of the burn, or the damage to the vegetation immediately after the fire. Often confused with the term burn *intensity* which refers to the level of heat produced and flame length, our definition of burn severity includes how thoroughly the vegetation was burned, regardless of the pre-existing fuel load.

This study hypothesizes that burn severity can be modeled with remote sensing techniques using either single date imagery or multi-temporal differencing incorporated with pre- and/or post-fire field data. A sub-study to this project includes testing the hypothesis that pre-fire fuel loads are correlated with burn severity levels.

1.2 Background

1.2.1 Remote Sensing

Remote sensing is the science of collecting data about a feature(s) on earth without being in physical contact with the subject of interest. Lillesand et al. (2004) describe it as the science and art of acquiring information about an object, area, or phenomenon by analyzing data that is acquired by a device not in contact with that which it is observing. Biophysical characteristics and human activities can be measured and monitored with this technology (Jensen, 2000). Images are taken of the earth's surface capturing energy (i.e. light) from the electromagnetic spectrum. The spectral composition of this radiated energy represents information about the physical properties of vegetation, soil, and water. Parts of the electromagnetic spectrum (i.e.

visible bands and infrared bands) are separated from the remaining data and analyzed using remote sensing software. The spectral information from the feature of interest is put into an interpretable form with remote sensing segmentations, techniques, and indices. We can detect change over time applying multi-temporal remote sensing techniques, which is comparing imagery from different time periods.

1.2.2 Remote Sensing of Vegetation in Semi-Arid Environments

Special remote sensing problems need to be considered in rangeland ecosystems due to the variability within the vegetation (or the lack of) and the presence and high reflectance of soil. These rangeland characteristics contribute to the unreliability of remote sensing of vegetation along with: nonlinear mixing due to multiple scattering of light, evolutionary adaptations (making desert plants spectrally dissimilar and lacking a strong red edge), spectral variability within the same species (due to spatially discontinuous precipitation patterns), open shrub canopies (affecting near infrared (NIR) reflectance), small plant canopies, and varying phenological status of plant canopies across space and time (Asner and Heidebrecht, 2002; Okin et al., 2001). Because there tends to be an abundance of bareground in sagebrush steppe rangeland ecosystems and soil reflectance is often brighter than vegetation reflectance, bareground 'dilutes' the vegetation signature. There are many vegetation indices used to detect vegetation parameters; however, problems exist with using these in rangeland ecosystems because they do not account for soil background variations (Qi et al., 1994). This phenomenon of soil influencing the interpretation of vegetation has been well documented (Bannari et al., 1995; Huete, 1988; Huete, 1989; Qi et al., 1994; Schmidt and Karnieli, 2001). It has also been shown that the

variation in soil brightness (i.e. wet vs. dry, and different soil association characteristics) can affect the results of vegetation indices (Schmidt and Karnieli, 2001; Asner, 2004). Examples of indices used in semiarid environments include the normalized difference vegetation index (NDVI), soil adjusted vegetation index (SAVI), and modified soil adjusted vegetation index (MSAVI).

The normalized difference vegetation index (NDVI; equation 1), attributed to Rouse et al. (1973), is a remote sensing technique used to estimate vegetation biomass. The NIR band of the electromagnetic spectrum make this measure sensitive to the physiological activity of plants and the red band is sensitive to vegetation and soil discrimination (Jensen, 2000). Though vegetation has been monitored on global scales using the NDVI, it is a poor indicator of vegetation biomass when vegetation cover is low, such as in semiarid rangelands (Huete et al., 1987; Schowengerdt, 1997). This index varies between negative 1 to positive 1.

$$\frac{NIR - Red}{NIR + Red} \qquad (1)$$

The soil adjusted vegetation index (SAVI) is a transformation technique which minimizes soil brightness and soil variations using the red and near-infrared wavelengths as well as a constant soil adjustment factor L. Huete (1988) found that an adjustment factor of 0.5 reduced soil noise across a range of broad-leaf cotton and narrow-leaf grass canopy densities. Huete determined that an adjustment factor of 0.5 could be used across different vegetation densities and different soil types.

The inductive modified soil adjusted vegetation index (MSAVI) is useful to detect vegetation in arid environments because of its ability to account for high bareground reflectance using a *variable* soil adjustment factor L (Qi et al., 1994). The

MSAVI remote sensing index uses an iterative inductive equation to calculate L. Furthermore, MSAVI iteratively calculates L until the soil cannot be minimized any more.

1.2.3 Remote Sensing of Burns and Burn Severity

The application of remote sensing for burned area analysis has increased recently utilizing several different sensors, resolutions, and techniques (Garcia and Chuvieco, 2004). Many studies have been performed in forested ecosystems to determine burn severity within a burn perimeter (Patterson and Yool, 1998; Wimberly and Reilly, in press; Turner et al., 1994; White et al., 1996; van Wagtendonk et al., 2004; Brewer et al., 2005; Epting and Verbyla, 2005; Epting et al., 2005), but few have been carried out specifically in areas with reduced vegetation cover (Smith et al., 2005; Roy et al., 2006) or specifically within semiarid sagebrush steppe ecosystems.

The traditional technique to detect burned areas and burn severity is by estimating biomass loss with the NDVI (Salvador et al., 2000; Flasse et al., 2004; Diaz-Delgado et al., 2003). However, bands in the visible spectrum can be susceptible to atmospheric interference and less sensitive to changes in burned landscapes than infrared bands. The NDVI was used until about 1999, when Lopez Garcia and Caselles (1991) developed an algorithm later coined by Key and Benson as the normalized burn ratio (NBR; equation 2) using Landsat imagery (Key and Benson, 1999b; Salvador et al., 2000; Key and Benson, 2004a; Key and Benson, 2006). Since then, it is the most widely used method on large fires (>500 acres) for perimeter and burn severity detection on public lands (Cocke et al., 2005; Key and Benson, 2006).

$$\frac{Band\ 4 - Band\ 7}{Band\ 4 + Band\ 7} \qquad (2)$$

Where: Band 4 = Landsat Band 4 (.76-.90 μm)

Band 7 = Landsat Band 7 (2.08-2.35 μm)

The NBR algorithm was developed in a mild-warm/subtropical climate study area composed of 2/3 forest and 1/3 scrub/bush using Landsat 5 (TM) (Lopez Garcia and Caselles, 1991). A correlation matrix of the reference and burned area was performed to determine the most uncorrelated pair of Landsat bands. The shortwave infrared (SWIR) band increases most after fire, and the near infrared band decreases most after fire. As a result, their technique uses the near-infrared and shortwave infrared bands because these bands correspond best with vegetation change due to fire in the forested ecosystem in which it was developed. Later the algorithm was put to ardent use by Key and Benson (1999b, 2004a, 2006) within forested ecosystems using Landsat TM/ETM+ imagery (NBR, equation 2). Landsat data have been traditionally used to map burned areas and fire severity (White et al., 1996; Patterson and Yool, 1998; Key and Benson, 1999b, 2004a; Santos et al., 1999; Salvador et al., 2000; Miller and Yool, 2002; Diaz-Delgado et al., 2003; Garcia and Chuvieco, 2004; Howard and Lacasse, 2004; van Wagtendonk et al., 2004; Brewer et al., 2005; Epting et al., 2005; Cocke et al., 2005; Roy et al., 2006). The NBR index is evaluated by correlating the index with field-based composite burn index (CBI) values. Performed in the field, the CBI was developed by Key and Benson (1999a, 2004b) as an ocular measurement of fire severity within each study plot that corresponds with sensor radiometric response data. CBI data include percent of foliage and litter/moss consumed, as well as percent of re-sprouting vegetation.

A differenced NBR (dNBR) is used to offer a quantitative measure of environmental change due to the fire, or temporal difference (Key and Benson, 1999b; Key and Benson, 2004a). The dNBR represents a scaled index of the magnitude of change caused by fire (van Wagtendonk et al., 2004). To do this, the post-fire NBR data set is subtracted from the pre-fire NBR data set (equation 3).

$$dNBR = NBR_{pre\text{-}fire} - NBR_{post\text{-}fire} \quad (3)$$

There are two types of dNBR severity measures, an initial assessment and an extended assessment. The initial assessment represents immediate change: the post-fire scene is acquired immediately after the fire. However, the extended assessment represents recovery of the plant community. The post-fire scene is not acquired until the next growing season, which could be as early as a few weeks or 11 months after the fire, depending on the season of fire (Key and Benson, 2004a). The pre-fire scenes for each assessment are taken within the same seasonal period, either the same year or an earlier year (to match phenological timing).

The NBR and dNBR may or may not be applicable in rangeland ecosystems due to vegetation re-growth times with respect to the seasonality of the burn. For instance, it takes longer for forested ecosystems to recover to pre-fire conditions (i.e., having the same reflectance) than rangelands. Alternatively, depending on pre-fire condition and the season of the burn in rangelands, vegetation can recover as early as the end of the same growing season, or as up to 10 years following the fire.

Several single date and multi-date approaches have been compared for the assessment of burn severity in forests such as those by Epting et al. (2005) and Brewer et al. (2005). Epting et al. (2005) evaluated 13 remote sensing techniques as

both single date and multi-date analyses including: three Landsat TM and ETM+ band ratios (bands 7/4, 7/5, 4/5); three vegetation indices (NDVI, SAVI, MSAVI); two multivariate transformations (a Kauth-Thomas Tasseled Cap transformation including greenness and wetness components, and Second Principal Components Analysis); normalized burn ratio (NBR; and differenced normalized burn ratio (dNBR)), and single TM bands 4, 6, and 7. Though Epting et al. (2005) had highest results (correlating field measures of fire severity with mapped fire severity) with the dNBR in forested areas, they determined that the dNBR may not be appropriate for estimating burn severity in non-forested areas. Brewer et al. (2005) compared six remote sensing indices: two principal components analyses; two artificial neural network classifications (a back propagation and a k-nearest neighbor); and two normalized difference indices (NBR and a modified NBR which replaced Landsat band 7 with band 5). Out of the six methods compared, Brewer et al. (2005) determined that the dNBR was the simplest method that does not introduce analyst input error (i.e., human bias) with the advantage that it can be used anywhere in the continental U.S. They separated forest (unburned, low severity, and high severity classes), shrub, and grass vegetation (unburned and burned classes), and resulted in 100% user accuracies for the burned/unburned shrub categories when compared with National Land Cover Data. Roy et al. (2006) agree that the dNBR is suboptimal in non-forested areas because of its insensitivity to burn severity. Miller and Thode (in revision) found that a Landsat relative dNBR (Table 1; RdNBR) performs better than the absolute dNBR at detecting high burn severity areas from moderate burn severity in a mixed forest/shrubland study area. Gerard et al. (2003) developed an algorithm

coined the normalized difference SWIR (NDSWIR; Table 1) to map fire scar burns using pre-fire and post-fire SPOT NIR (0.84 μm) and SWIR (1.66μm) bands. The SPOT SWIR band is useful for the detection of old fire scars and canopy moisture content (Gerard et al., 2003).

1.3 Study Area

This study takes place within the Hitching Post pasture, a 3.24 km^2 fenced parcel within the U.S. Sheep Experiment Station (USSES) located in Clark County, Idaho at an elevation of approximately 1800 m (Fig. 1). Average annual precipitation ranges from 250-530 mm with up to seventy percent falling as snow (Seefeldt, 2005). Average annual temperatures are 5-6 °C, with a 70 to 90 day frost-free season. The majority of the pasture has gradual slopes (0-1.5 %), with the greatest slope being approximately 9 % excluding rocky outcrops. The pasture is a sagebrush steppe ecosystem characterized by extreme seasonal variability and a co-dominance of *Artemisia* with several grass species (West and Young, 2000). The Hitching Post pasture has two primary subspecies of sagebrush (*Artemisia* ssp.): mountain big (*A. tridentata* ssp. *vaseyana*), and threetip (*A. tripartita* ssp. *tripartita*). Mountain big sagebrush is a more mesic subspecies located between 1525 m and 3050 m elevation (Wright and Bailey, 1982). It is between 0.73 - 1.22 m tall in precipitation zones varying between 355 - 510 mm per year. Threetip sagebrush is typically found below 1830 m in dry soils receiving between 255 - 400 mm of precipitation per year (Wright and Bailey, 1982). This subspecies is a weak sprouter (grows from the meristem). Other shrub species within the pasture are antelope bitterbrush (*Purshia tridentata*), green rabbitbrush (*Chrysothamnus viscidiflorus)*, and horsebrush (*Tetradymia*

canescens). There are a few small patches of the exotic forbs leafy spurge (*Euphorbia esula*) and spotted knapweed (*Centaurea maculosa)*. The exotic annual, cheatgrass (*Bromus tectorum)*, occurs as a small component (<1%) of the overall plant cover. Lupine (*Lupinus argenteus)* is the most plentiful forb in the pasture, ranging in height from 20 cm to 1 m; graminoids present are thickspike wheatgrass (*Elymus lanceolatus)*, bluebunch wheatgrass (*Pseudoroegneria spicata*), and plains reedgrass (*Calamogrostis montanensis* Scribn.). Soils are mixed, fine-loamy, frigid Calcic Argixerolls derived from residuum, alluvium, or windblown loess (Seefeldt, 2005; NRCS, 1995). Sheep and horses have grazed this pasture for the last decade, but grazing has not occurred for the past 2.5 years prior to the burn.

This study area was chosen because it offered an opportunity to participate in a prescribed burn, allowed a high degree of control for pre- and post-fire field sampling, and because it contained a sagebrush steppe rangeland environment. The prescribed burn occurred September 23 and 24, 2005, and is described in more detail below.

2.0 Field Methods

2.1 Introduction

This study utilizes pre- and post-fire field-based sampling as training sites for establishing locations of sample sites along with a description of the vegetation, bareground, and burn severity observed at each site. The pre-fire field assessments were collected by two people together between mid-June and early August 2005, and post-fire sampling followed the September 2005 prescribed burn for approximately

1.5 months. Burn severity is assessed using a combination of field and satellite data that evaluate the vegetation lost due to fire. These field vegetation estimates are compared with remote sensing data with the goal to delineate areas of high and low amounts of live vegetation cover post-fire. The parameters we use to determine burn severity in the field are: 0% = no area burned, <50% = <50% area burned, >50% = >50% area burned, and 100% = all area burned.

Prior to the vegetation surveys, large-scale (~8000 m^2) vegetation variability and fuel load estimates were performed across the pasture to design a sampling regime which adequately sampled across all fuel loads. Fuel loads were sampled to get an accurate representation of pre-fire vegetation communities. Because the vegetation communities (i.e. fuel load and species type) were similar on all soils, elevations, and aspects in the pasture, further stratification of sampling was not necessary. Upon walking the entire pasture, three main types of vegetation cover (fuel load) were observed. There were patches of grass only (with bareground); patches of small, sparse shrubs (with grass and forbs); and patches of tall, dense shrubs (with grass and forbs). These qualitative observations are based on the work of the BLM's Determining Fuel Models method, which ocularly estimates the vegetation across a shrubland landscape in tons/acre (Anderson, 1982). Though biomass measurements are never made, this technique estimates biomass visually based primarily on grass and shrub (size and density) cover in rangelands. According to a USDA fuel load guidelines study, Anderson (1982) found that grass-only parts of shrublands equate to less than 1 ton/acre, and their shrublands averaged 4 tons/acre. Our fuel load categories correspond with Anderson's observations: grass-only patches are

considered very low fuel load while high fuel load is characterized by tall, dense shrub areas. A transitional category of medium was formed, which is small to medium-sized shrubs with grass and forbs. During this process, 78 polygons ~8267 m^2 each (with consistent fuel loads) were recorded with a Trimble GeoXT GPS receiver (+/- 0.7m @ 95% CI (Serr, unpublished)) and labeled with their respective fuel loads. These polygons are hereafter named 'large scale, homogenous fuel load polygons'.

After the large-scale fuel load estimates were performed, two different methods for fine scale sampling of the vegetation were performed. These include: 1) 60 m x 60 m plot ocular estimates of vegetation and bareground percent cover, and 2) 20 m x 40 m plot point frame measurements. The ocular method is used for quickly collecting percent cover of the upper-most canopy and comparing the results with remote sensing data. Percent cover of shrub, grass, forb, litter, rock, and bareground are estimated over a 60 m x 60 m plot, after thoroughly walking the area. The point frame method takes longer in the field; however, it provides a more accurate representation of true ground cover (Floyd and Anderson, 1982; Floyd and Anderson, 1987). The point frame method was used because: 1) it serves as a complimentary method for coupling ground data with remote sensing data; 2) it provides fine resolution field data roughly equivalent to the resolution of the SPOT imagery (10 m); and 3) the near-nadir view while sampling the vegetation emulates the view of a satellite.

2.1.1 Pre-Field Operations

ESRI's ArcPad, (6.0.2, 1990-2000), a mobile GIS software installed on the GPS unit allowed seamless data collection between GPS locations and field attributes. ArcPad Application Builder in ArcPad Studio (6.0.0.24U, 2002) was used to customize an attributed form associated with each shapefile collected in the field. Pre-established categorical groups were used to assess percent cover (Table 2) for each cover class (shrub, grass, litter, bareground, rock, and forb) (McMahan et al., 2003).

2.1.2 Field-Based Ocular Estimates

The ocular estimate method used was developed by the ISU GIS Training and Research Center (TReC) and modified by McMahan et al. (2003) for semiarid rangelands in southeastern Idaho. Plots are approximately 60 m x 60 m in order to encompass approximately four Landsat pixels (30 m x 30 m). This method has been used by the TReC as a cover method for remote sensing interpretation/classification since 1999 (McMahan et al., 2003; Russell and Weber, 2003; and Weber and McMahan, 2003). Two hundred random sampling locations were generated using the Raster Drilldown tool (GIS TReC, 2006) across the pasture that met the following criteria: 1) >20m from all bulldozer-created black-lines (for enclosure of the prescribed fire), and 2) >20m from all roads to ensure roads were not within plots, to mitigate 'road effects', and to eliminate sampling bias. Six additional plots were created in order to have adequate replication within unburned areas and fuel load classes. These 60 m x 60 m ocular estimate plots were located within all fuel load categories and adequate (≥ 30) representation was insured for each category. In total, 206 ocular plots were navigated to using the GPS receiver. Each person started in the

plot center and paced 30 m in opposite directions to the plot boundary. After walking the plot circumference, they proceeded to walk in a spiral pattern within 3-4 m of the previous track back towards the plot center while observing plot attributes (Table 3). At the center, each plot attribute was discussed until agreed upon. Percent cover for six categorical categories (shrub, grass, forb, litter, rock, and bareground) were estimated. Each plot center location was recorded using the GPS receiver, and here sagebrush was described by its average height and diameter using calipers (+/-1cm) to approximate the age of each plant (Perryman and Olson, 2000). Four photo points were taken as well from the plot center, one in each cardinal direction. This method also includes identifying the dominant weed and estimating its abundance (percent cover). Fuel load (tons per acre) was estimated following BLM protocols (described above) over the 60 m x 60 m plot. Homogeneity of vegetation cover was assessed across each plot, and a plot was considered homogeneous if vegetation type and percent canopy cover was consistent at visually-based 10 m^2 increments across an entire plot. Therefore, if a 10 m^2 portion of the plot was different than the remaining areas within a plot, then the plot as a whole was not considered homogenous.

2.1.3 Field-Based Point Frame Measurements

Because the study uses 10 m SPOT imagery, a finer scale field method (versus the 60 m plot estimates) was sought for comparison with the imagery. Thus we chose point frame measurements made over a 20 x 40 m plot size which can encompass eight SPOT pixels. This plot size allows a benefit over a smaller plot size because there are more pixels in the plot tolerating some georegistration error. Though ocular estimates are time efficient and easy, they can be less precise (than point or line

methods) and inherently subjective. In addition, the somewhat coarse and unequal (~ 14%) categorical increments (Table 2) used can be difficult to relate to absolute remote sensing measurements. It is important to determine a field method that is applicable to remote sensing in rangelands, and furthermore that is reliable, user-friendly, and lacks user bias. Because the field data are an integral part of remote sensing models, it must be accurate enough relative to the imagery resolution. It is important to note; however, that because exact vegetation coverages are unknown (using plots due to the time constraints of collecting cover across the whole study area), it is difficult to compare coverage techniques with absolute certainty.

The point frame technique, designed by Floyd and Anderson (1982) is a well accepted, accurate sampling method used to visually determine vegetation percent cover (Floyd and Anderson, 1987; Inouye, 2002). Designed in sagebrush steppe ecosystems, this frame establishes a dot grid overlooking underlying vegetation and bareground. Observers view vegetation from a near-nadir standing position and record the cover types that are beneath 36 intercepted points (cross-hairs). A number of point frames are collected within each pre-defined plot size; the sampling intensity necessary to capture variability within each plot was determined using a sample effort curve (Fig. 2). Based on sample effort curves from all cover categories, a maximum of 15 frames of point data were needed at each plot to ensure adequate representation of ground cover in this study area. The location of the 15 frames within each plot were selected at 7 m intervals across the 40 m-axis of the plot, then placed at 3 m, 5 m, and 7 m perpendicular to each interval along the 20 m-axis (Fig. 3). The 20 x 40 m plot boundary was established with a field tape and recorded with the GPS. In

addition to the ground cover class identified (at each cross-hair) in the frame, fuel load (tons per acre) was estimated following BLM protocols (same as above), and homogeneity was assessed at the 20 m x 40 m scale. Each plot's attributes (Table 4) were entered into the GPS.

2.2 Field Methods--Sampling Stages

2.2.1 Pre-fire Sampling

Pre-fire ground cover sampling was performed primarily for hypothesis #2 to determine correlation between pre-fire fuel loads and burn severity levels. During pre-fire sampling, the ocular estimate method was performed at 206 random plots across the pasture (Fig. 4; points). In conjunction with the ocular estimates, point frame data (Fig. 4; rectangles) were collected at 45 of the 206 sample sites. These 45 plots were centered within the ocular plots that were determined homogenous. In order to ensure replication, 20 additional stratified random point frame plots were set up within the previously established large scale, homogenous fuel load polygons. Each of the three fuel load categories were represented by at least four, 20 m x 40 m point frame plots and four plots were established within the proposed unburned area for replication.

2.2.2 Prescribed Fire

The prescribed fire was performed September 23 and 24, 2005 by Targhee Fire, a contract crew through the USSES. The fire crews burned most of the northern 4/5 of the pasture (approximately 2.82 km^2; Fig. 4) consistently. They ignited vegetation in the southeast and northwest corners simultaneously while walking the dozerline with a drip torch towards the southwest corner. These two fires came

together in the southwest corner and progressively moved toward the northeast with the wind. Using a hand-held anemometer, winds were observed around 20 m/sec throughout most of this northern burn. Nine strip burning/spot fires were ignited in the southern portion of the pasture to ensure replication (south of the middle bulldozer line; Fig. 4). The prescribed fire in September burned approximately 85% of the pasture area including 173 of the sampling sites.

2.2.3 Post-Fire Sampling

Post-fire field surveys, performed within 1.5 months after the fire, were intended to provide field validation of burn severity levels. All of the pre-fire sampling sites were re-sampled after the fire. The same field methods as pre-fire sampling (ocular estimates and point frame measurements) were repeated at the same scales and within 3-5 m of the original locations (by navigating with the GPS unit). Data were collected consistent to the pre-fire methods, except fuel load attributes and sagebrush age data. In addition, a burn severity rating (unburned, low, moderate, and high) was assigned to each ocular and point frame plot. This project assessed burn severity with a modified ocular method based on combining the works of the US Forest Service field methods (USDA FS, 2001), the US Park Service field methods (USDI NPS, 2003), and Key and Benson's (Key and Benson, 1999a; 2004b) composite burn index (CBI). Each of these post-fire field methods incorporates qualitative and quantitative measurements to detect and categorize burn severity; we incorporated and modified the three methods above according to the burn conditions on our study area in the context of a semiarid rangeland site. Since most of the vegetation and organic soil material was consumed by the fire the burn severity

assessment became solely qualitative; no attribute was physically measured. However, attributes such as litter condition, shrub condition, surface rock (USDA FS), organic substrate, and vegetation (USDI NPS) were incorporated from the USDA and USDI burn severity assessments. Key and Benson's (1999a; 2004b) CBI places a ≈50% change in the herb/low shrub/tall shrub strata into the moderate burn severity category. The study area predominantly fits into Key and Benson's shrub strata, so we incorporated this ≈50% change burn severity category.

After the burn, we walked the entire pasture to assess the burn severity variability using the attributes that were applicable to the prescribed burn. For instance, we did not use any tree measurements (there were no trees) or measurements of standing litter (all burned areas had standing burned stumps). In most instances, the fire either burned all vegetation (except stumps) or none; there was a very small amount of incompletely burned vegetation.

Severity at each plot was assessed based on the percent cover of consumed, above-ground vegetation and litter versus the amount of bareground and rock, as a satellite would interpret each plot's reflectance. If there were patches of partly consumed vegetation within the plot its percent cover was assessed and a severity category was assigned. Each study plot was classified with an ocular burn severity rating (0-3) based on the amount of remaining above-ground live vegetation within the plot: 0 = Unburned, no vegetation change; 1 = <50% burned, little above ground consumption; 2 = >50% burned, most of above ground vegetation was consumed; and 3 = 100% burned, all above-ground vegetation mortality. Of 271 total plots, only 13 were <50% burned. The corresponding remote sensing values were not significantly

different than the unburned or moderate severity classes and there were not enough plots for validation. These data were incorporated and analyzed with the >50% category (2) (see Table 5) because the sample size was too low to have its own class and subsequently considered moderate severity or 'incompletely burned'.

2.2.4 Post-Field Operations

Differential correction/post processing was performed to minimize clock (satellite and receiver), atmospheric, and ephemeris errors of the GPS data. Trimble's GPS Pathfinder Office 3.10 was used for differential correction and shape correct. The real time CORS stations located in Mammoth, WY and at the Idaho National Laboratory (INL) (depending on which was available) were preferred for the differential correction. However, when necessary, CORS stations located further away (i.e. Pocatello, ID) were used.

3.0 Remote Sensing Methods

3.1 Image Acquisition

Landsat ETM+ and SPOT 5 imagery were chosen for this work due to their reasonable cost, spatial and spectral resolution, and because their data are continuously collected. Both Landsat and SPOT satellite images were acquired within one month after the prescribed fire. Landsat has three visible (blue, green, red), one near-infrared (NIR), and two shortwave infrared (SWIR) bands (1.65 μm and 2.21 μm) at 28.5 m spatial resolution. While Landsat provides more spectral resolution (especially in the SWIR where burn severity is likely to be distinguishable), the spatial resolution is lower than SPOT-5 and its long-term future data availability is

questionable. SPOT-5 has three multispectral bands (green, red, and NIR) at 10 m spatial resolution and one SWIR band (~1.66 μm) at 20 m spatial resolution. Because the SPOT SWIR band has a spatial resolution of 20 m and the visible and NIR data have a spatial resolution of 10 m, the SWIR data were resampled to 10 m and analyzed together with the visible and NIR data. A total of 2 Landsat (July 4 and October 24, 2005) and 2 SPOT (August 27 and September 28, 2005) images were acquired (Table 6): all images were chosen as close to the prescribed burn (September 23 and 24, 2005) as possible with the smallest percentage of cloud cover.

3.2 Overview of Image Processing

Several remote sensing methods are explored and compared in this study using Landsat and SPOT imagery. In order to test the hypothesis that burn severity can be predicted with remote sensing data, ten remote sensing indices are explored and compared through accuracy assessments. The indices include: 1) an original Landsat dNBR and one relative dNBR using pre- and post-burn imagery; 2) one relative modified NDVI using pre- and post-fire imagery; 3) one original normalized difference shortwave-infrared index (NDSWIR), and two modified NDSWIR using multi-imagery and post-fire imagery; 4) two SAVIs using an adjustment factor of 0.5 with both the Landsat and SPOT post-fire images; and 5) two MSAVIs using post-fire Landsat and post-fire SPOT imagery.

Using homogenous point frame study plots (n=36) we investigated the differences in the pre- and post-fire SPOT and Landsat images (Figures 5 and 6). We averaged the reflectance values from the 36 plots for each of the pre- and post-fire images and compared the differences. The SPOT data had small changes in

reflectance values between the pre-and post-fire images. The red reflectance decreased after the fire approximately 0.84% and the NIR reflectance increased approximately 1.8% after the fire. The green reflectance increased 1.6% and the SWIR reflectance increased approximately 0.81%. In the Landsat data the NIR decreased 3% and the SWIR (2.21 μm) reflectance increased 5.5% after the fire. Blue, green, and red reflectances decreased less than 1% and the SWIR (1.66 μm) increased 0.85%.

Interpretation of the reflectance values from the homogeneous plots indicates that the SPOT data demonstrate a smaller amount of change between pre- and post-fire in comparison to the Landsat data. The post-fire Landsat data was collected approximately one month after the fire while the SPOT data was collected 4 days after the fire. The Landsat post-fire response (a decrease in NIR reflectance and an increase in SWIR reflectance) is consistent with a loss of vegetation and an increase in soil exposure. On the other hand, the SPOT green and NIR reflectances increased, albeit less than 2%. The response of the SPOT data in the red and SWIR bands is similar to that of corresponding bands in the Landsat data. Regardless of the green and NIR increases, we chose to analyze the SPOT data and compare results with Landsat.

Because resource management decisions are made with maps it is important to know their quality of information. Accuracy assessment is conducted to identify how well the remotely sensed data represents earth's features and provides a measure of quality that remotely sensed data describes of land cover (Congalton and Green, 1999). Validation of the remote sensing burn severity was performed following

traditional accuracy assessment techniques by placing field data (reference data) and remote sensing data (classified data) into an error matrix (Congalton and Green, 1999). The standard error matrix reports users, producer's, and overall accuracies, as well as a kappa statistic (KHAT). The overall accuracy, reported as the accuracy assessment statistic, is the sum of the correctly classified pixels divided by the total number of pixels in the error matrix (see below; Congalton and Green, 1999). Producer's and users accuracies are a better representation of accuracy because they represent the individual category accuracies, and are not biased by the overall sample size. The producer's accuracy reports the percentage of pixels which accurately represent the landscape (on the map). The users accuracy represents the chances of, when going to an area on the ground, that the map will be classified correctly. The KHAT is a measure of how well the remotely sensed data agree with the validation data and provides insight into how much better the classification is than a random classification (Congalton and Green, 1999).

A pairwise test of significance (Congalton and Green, 1999; equation 4) was run for the matrices that had highest accuracies as well as for those which shared similar overall accuracies. This test is a Kappa analysis that determines if two error matrices are significantly different by comparing their KHAT statistics.

$$Z = \frac{|K1 - K2|}{\sqrt{\text{var}(K1) + \text{var}(K2)}} \qquad (4)$$

Where: K1 and K2 = Kappa statistic for error matrix 1 and 2

var(K1) and var(K2) = estimates of variance for matrix 1 and 2

3.3 Pre-processing of Imagery

3.3.1 Radiometric Correction

All imagery were processed to at-satellite reflectance using ENVI software (RSI, 2005) to reduce between-scene variability. This was an important step since multi-temporal imagery was used. Both Landsat images were processed using ENVI's Landsat TM Calibration Utility; the SPOT images were processed using band math in ENVI with algorithms (4) (SPOT, 2005) and (5) (Landsat 7, 2006) as follows:

$$\text{Radiance} = \frac{\text{Digital Number}}{\text{Absolute Calibration Gain}} \quad (5)$$

$$\text{Reflectance} = \frac{\Pi * \text{radiance} * \text{sun-earth distance}^2}{\text{solar equivalent irradiance} * \cos(\text{solar angle})} \quad (6)$$

Where: *Radiance* = spectral radiance at the sensor's aperture

Digital Number = the digital number of each pixel ranging from 0-255

Absolute Calibration Gain = the sensor processing procedure to maximize the instrument's radiometric resolution without saturating the detectors; each band's gain is provided by the image metadata

Sun-Earth Distance = Earth-Sun distance in astronomical units from nautical handbook

Solar Equivalent Irradiance = mean solar exoatmospheric irradiances in watts/(meter squared * μm) provided by SPOT Image Corp. for each band

Solar Angle = solar zenith angle in degrees

On May 31, 2003 the Landsat ETM+ scan line corrector (SLC) which compensates for forward motion of the spacecraft failed (Howard and Lacasse, 2004). This mechanical failure cannot be repaired, thus, portions of the ground are collected redundantly or missed entirely. While a linear transform of the data from another scene date can be used to estimate the missing DN values (Howard and Lacasse, 2004) this was not necessary because our study area was not located in an area affected by the SLC failure.

3.3.2 Geometric Correction

Image rectification was performed using ground control points (GCPs) and the Image to Map Registration tool in ENVI. Image rectification was performed after the remote sensing indices (see below) in order to reduce error during resampling. Spatial interpolation was performed using GCPs selected from the index images and matched with the primary 'Dozerline' GPS GCP file. This GPS file was collected around the periphery of the controlled burn, which could easily be matched with the burn periphery in the index images. Where necessary, GCPs from roads and pasture corners were also used. Both the GCP files and index image files were in a Transverse Mercator projection (SPOT = IDTM; Landsat = UTM) and the GCPs were located spatially throughout the study area. Each image was then subset to the study area.

Resampling during the image rectification process was implemented using the nearest neighbor first order polynomial interpolation. The output pixel size was set to the same size as the input image file. This method was chosen because it assigns the closest brightness value to the output pixel, rather than an average of the surrounding pixels (Jensen, 1996; Lillesand et al., 2004), therefore maximizing spectral and spatial integrity of the data. The resulting Root Mean Square Error (RMSE) was less than ½ pixel for both the Landsat and SPOT imagery (Table 7) during the image rectification process.

3.4 Remote Sensing Indices

Several remote sensing indices were implemented (Table 1) including single image and multi-image manipulation. A burn versus no burn algorithm was first sought to differentiate the areas that were burned from the areas that were not burned. Subsequently, an algorithm was sought to determine areas of differing levels of burn severity. There is a possibility of introducing inherent error when comparing multi-temporal datasets and using them in band ratios due to spatial mis-interpolation, therefore; single image segmentation was performed to reduce this occurrence. Multi-date indices were performed in order to show change detection from pre-burn conditions to post-burn conditions. This temporal image differencing technique uses the same bands from each image; the same algorithm is applied twice for each image; and the post-fire result is subtracted from the pre-fire result. Algorithms compared with Landsat imagery were: soil adjusted vegetation index (SAVI) and modified soil adjusted vegetation index (MSAVI) single date indices, and differenced normalized burn ratio (dNBR), normalized difference SWIR (NDSWIR), and relative dNBR

multi-date images. Algorithms compared with SPOT imagery were: SAVI, MSAVI, and post-fire NDSWIR single date indices, and relative modified normalized difference vegetation index (NDVI) and NDSWIR multi-date indices.

3.4.1 Single Date Indices

Single date indices represent change by using only the post-fire satellite image. For initial assessment of burn severity, it is best to use imagery as close after the fire date as possible. The Landsat and SPOT post-fire images were used to produce three remote sensing indices: SAVI, MSAVI, and NDSWIR. These single date indices were applied to determine burned from unburned areas, and then assessed to differentiate burn severity.

The SAVI remote sensing index was appropriate to try in our rangeland application with both the Landsat and SPOT post-fire images because of the inherent amount of high bareground after a fire. Huete (1988) suggests that a soil adjustment factor of 0.5 can be used across different ecosystem types with differing biomass amounts. The SAVI output values range between 0-1: values near zero represent less vegetation (high burn severity) and increasing values represent more vegetation (low burn severity or unburned vegetation).

The MSAVI was used (with Landsat and SPOT post-fire images) because it has increased sensitivity to vegetation where total vegetation cover is low (i.e. after a fire) (Qi et al., 1994). The MSAVI output values range between -1 to 1. It is expected that this algorithm is successful at discriminating vegetation associated with unburned and moderate severity burns because of its ability to minimize soil's high reflectance.

We chose to assess the accuracy of the post-fire NDSWIR (pNDSWIR), described in better detail below. This index uses SPOT NIR and SWIR bands and no visible bands; therefore, potentially less susceptible to atmospheric interferences.

3.4.2 Multi-Date Indices

Multi-image manipulation was first performed to identify burned from unburned areas and then to differentiate burn severity levels within a burn perimeter. This process detects vegetation change from pre-burn to post-burn conditions using two images. Typically multi-date indices require an algorithm to be applied to both pre-fire and post-fire images before the final algorithm is performed (i.e. differenced). Areas of no change have values equal to, or close to zero. For instance, a pre- and post-NBR is performed and then differenced resulting with the dNBR (Table 1). As established, Landsat bands 4 and 7 are applied in the dNBR with values typically ranging from negative 1 to positive 1; negative values represent increased vegetation productivity in the post-fire scene or clouds in the pre-fire scene, positive values represent fire effects or clouds in the post-fire scene. We applied a dNBR to the Landsat data.

We also used Landsat data for a relative differenced NBR (RdNBR; Miller and Thode, in revision). RdNBR values range from -1 to 1; negative values represent increased vegetation (unburned or low severity), and positive values represent a decrease in vegetation (high severity) after the fire. The relative dNBR was not used with SPOT data because the pre-fire NBR results have negative values and this index requires the division of the square root of the pre-fire NBR results. Therefore because the pre-fire NBR has negative values it cannot be performed without scaling the pre-

fire data to positive values. The aim of this research was to test indices without additional need of processing (e.g. rescaling).

The NDSWIR results are compared with the results of the post-fire pNDSWIR (above). Because spectral proximity of the Landsat band 5 (1.65 μm) is similar to SPOT's SWIR (1.66μm), the NDSWIR index (Gerard et al., 2003) was modified to include the Landsat imagery. It was expected that the Landsat and SPOT NDSWIR indices would have similar results because of the SWIR bands' spectral proximity. However, because the SPOT spatial resolution is higher than the Landsat spatial resolution, it was expected that the SPOT NDSWIR may provide an increased level of delineation.

To incorporate SPOT's SWIR band, the NDVI was modified by replacing the NIR with the SWIR band which was previously found useful for fire scar detection (Gerard et al, 2003). We performed the modifiedNDVI (Table 1) with the pre-fire and post-fire SPOT images in order to produce a relative modified NDVI index (rModNDVI).

Accuracy assessment (described below) was used to provide an assessment of how well the remotely sensed indices corresponded with the field data. Accuracy results were then compared between the 10 remote sensing indices.

4.0 Accuracy Assessment

4.1 Relating Remote Sensing Indices to Field Data

Training data were used to relate remote sensing index values to field data. Using field plot data and the Spatial Analyst function in ArcMap 9.1 (Extract Values

to Points; ESRI, 2005) burn severity index values were extrapolated for each training plot. The Extract Values to Points function acquires the pixel value under the plot center point. The Interpolate Values at Point Locations option was checked in order to account for the surrounding plot size. The value of the point is calculated using the adjacent cells with a bilinear interpolation method (ESRI, 2005). Burn severity index values were separated into burn severity classes by first placing all plot values into their respective burn severity classes as determined in the field. Then the minimum, maximum, and mean index values of each class were determined. Overlapping index values were separated by splitting the difference between the maximum of one class with the minimum of the next class. Likewise, if there was a gap between burn severity class data values, then a break was determined by splitting the difference between the maximum of one class with the minimum of the next class. A total of 119 plots were used for the training including both ocular and point frame plot index values. High burn severity had 89 plots; moderate burn severity ('incompletely burned') had 16 plots; and the unburned class had 14 plots. To encompass the variability across the study area, training plots were randomly selected within each burn severity class and the same training plots were used within each burn severity class for each index. A categorical scatterplot of burn severity classes and remote sensing index values was created to show the breaks and overlap in the remote sensing data (Fig. 7).

4.2 Validation

Fifty plots were reserved for the validation of each class (n=150), as recommended by Jensen (1996) (Table 8). No training data were used in the

validation. An error matrix was created to compare the field validation plots with their corresponding index values. Overall accuracy, as well as the users and producer's accuracy are presented in the error matrix table (Table 9). Error matrices for all ten remote sensing indices were established and Kappa analysis was performed. A pairwise test of significance was run for the matrices that had highest accuracies as well as for those which shared similar overall accuracies.

5.0 Results

The remote sensing indices comparing burned with unburned areas had better overall, users, and producer's accuracies than indices comparing burn severities (Tables 10, 12 - 14). Based on a homoscedastic, two-tail t-Test comparing the overall accuracies of 10 single date and 10 multi-date indices (with SPOT and Landsat data), the single date and multi-date indices do not differ in mean overall accuracy ($P = 0.4073$).

5.1 Burn Versus Unburned Index Results

Landsat remote sensing indices of dNBR, NDSWIR, MSAVI, SAVI, and RdNBR, and SPOT indices of dNDSWIR, pNDSWIR, rModNDVI, MSAVI, and SAVI were compared using all field data for accuracy assessment. The burned versus unburned indices generated using SPOT imagery (pNDSWIR, rModNDVI, and MSAVI), and the Landsat-derived burned versus unburned indices (dNBR, RdNBR, MSAVI, and SAVI) had relatively consistent results (~ 95% overall accuracy). Three burned vs. unburned SPOT-derived indices (pNDSWIR, MSAVI, and SAVI) have 95% or better overall accuracies (Table 10). The highest overall accuracy for the burn

vs. unburned indices was the SPOT SAVI at 100% (Table 11). The pNDSWIR had an overall accuracy of 96% and had a slightly higher KHAT value than the MSAVI results. Upon performing a pairwise test for significance between the pNDSWIR and MSAVI SPOT error matrices, the z-statistic (Z = 0.599) reveals that they are not significantly different. Three burned vs. unburned Landsat indices (RdNBR, MSAVI, and SAVI) performed nearly equally well at 95% overall accuracy (Table 12). Table 12 reports the same values (to the 100^{th}) of KHAT, variance, and z-statistics for these three indices, indicating they have equal classification accuracies (Congalton and Green, 1999); therefore, a pairwise test for significance is not necessary. The z-statistic values indicate that all three indices were significantly better than a random result. The remote sensing indices that assessed burned versus unburned areas had better overall, users, and producer's accuracy results than those detecting burn severity.

5.2 Burn Severity Index Results

The best burn severity index (differentiating unburned, moderate, and high) was the Landsat RdNBR with a 73% overall accuracy and users and producer's accuracies of 56% and 61%, respectively, for the moderate category and 76% and 63%, respectively for the high category (Table 13). The best overall accuracy for the SPOT burn severity indices was the SAVI index at 71% (Table 14). The pNDSWIR index closely followed at 69% and a pairwise test for significance (Z = 0.381) revealed that the two matrices are not significantly different. Z statistics indicate that all Landsat and SPOT indices (except the dNDSWIR) had significantly better results than if randomly classified.

6.0 Discussions and Conclusions

While studies have been performed in forested ecosystems to reliably detect burn severity with remote sensing data, there have not been any established in sagebrush steppe rangelands. This study compares the results of 10 remote sensing indices to delineate burned areas and burn severity within rangelands immediately following a fire using medium resolution satellite imagery. We used bands in the electromagnetic spectrum that correspond with vegetation change after a fire and algorithms sensitive to high reflectance of bareground that occurs in rangelands. It is important to note that overall accuracy cannot be relied upon completely because it can be biased by large sample sizes of one category versus another. For instance, the unburned results have much higher accuracies than the other burn severity classes resulting in inflated overall accuracies. As indicated by the highest users and producer's accuracies, the best index for determining burned from unburned areas was the SPOT SAVI (100% users and producer's accuracies for all categories) and the best index for differentiating burn severity within a burn was the Landsat RdNBR.

Consistent with Sannier (1999), Epting et al. (2005), and Miller and Yool (2002) accuracies were better with fewer burn severity categories. In all cases (except the SPOT dNDSWIR; Tables 10 and 13) the unburned versus burned indices had better results than the burn severity indices. We were able to successfully determine if an area was burned or not in rangelands using the SPOT pNDSWIR, rModNDVI, MSAVI, and SAVI indices and the Landsat dNBR, RdNBR, NDSWIR, MSAVI, and SAVI indices.

Our best burn severity index, the Landsat RdNBR (Fig. 8), supported Miller and Thode's (in revision) results. In a mixed ecosystem study area, they concluded that this index performed better at separating high burn severity from other burn severity classes. Our moderate and high burn severity users (56%, 76%, respectively) and producer's (61%, 63%, respectively) accuracies for the RdNBR were higher than all other indices. These results are important to land managers given that high severity areas require more recovery effort. Therefore, there is a need for high producer and user's accuracies in high severity areas (Miller and Thode, in revision).

Mapping burn severity patterns at a scale that is coarse enough to capture landscape scales for management, yet fine enough to provide the spectral differentiation between burn severity classes is needed. Though we did not test spatial variables between Landsat and SPOT, we can compare results of indices used on each dataset. For example, in comparing the NDSWIR, the SPOT index provides more spatial detail and morphology of the burn categories (Fig. 9). Therefore, even though SPOT didn't provide as high accuracies as the Landsat RdNBR for burn severity levels, its spatial resolution may provide other attributes that are useful to land managers. Landsat provides a practical scene size of 170 x 183 km and costs are reasonable if more than one image needs to be purchased. The results of the Landsat RdNBR verify that the Landsat 30 m spatial resolution is high enough to capture the spectral variability between burn severity classes in rangelands. However, it is up to the land manager to decide the level of detail needed to determine burn severity and thus the scale of fire recovery efforts.

Spatial correlation of ground cover and low RMS error (less than ½ a pixel) reduce the likelihood of classification error, however, they do not excuse the possibility of error. Therefore, although error is introduced with multitemporal data sets and spatial mis-interpolation occurs, these effects did not significantly alter the overall accuracies.

Timing of imagery acquisition is important in relation to the fire date and field sampling due to phenological vegetation changes. It is difficult to fairly compare remote sensing index results when timing of pre-fire and post-fire data sets vary. Naturally, a data set with more time between images will translate to more change in the index value. Our Landsat imagery had 112 days between the pre-fire and post-fire scenes as well as approximately 1 month between the burn and post-fire image, whereas the SPOT imagery had 32 days between imagery and only 4-5 days between the burn and post-fire image. Images acquired closest after a fire will likely show more immediate fire effects than images acquired for sometime after the fire. The multi-temporal indices between Landsat and SPOT carry different relationships. The shorter time gap between SPOT images and their acquisition dates (close to field data collection) coupled with the increased spatial resolution explains, in part, why the SPOT NDSWIR accuracy is slightly better than the Landsat NDSWIR. The higher sensitivity of the Landsat bands explains the higher accuracies for the burn severity levels. Recovery time is different in forests and rangelands and often depends on seasonal timing of fire. This should be considered when collecting imagery in order to model effects specific to fire.

In the pre-fire images, the SPOT and Landsat reflectance values are essentially the same (where their bands overlap). However, in the post-fire images, the SPOT and Landsat data differ. The green and NIR bands increase in the SPOT post-fire image (only four days after the fire) while the green and NIR Landsat bands decrease. The Landsat data is consistent with an increase in soil exposure and a loss of vegetation cover. On the other hand, the SPOT post-fire reflectances are counter-intuitive to an increase in soil exposure and a decrease in vegetation cover. These differences are most likely due to sensor characteristics (i.e. sensor angle, sun angle, and acquisition time) rather than data collection windows. The SWIR 1.66 μm data is essentially the same between the SPOT and Landsat pre- and post-fire data. The fact that Landsat provided a better discrimination of burn severity is likely due to the better spectral resolution (e.g. inclusion of the longer-wave SWIR band (band 7, 2.21 μm) and less importantly the blue band (band 1)). This result is expected as the longer SWIR bands are notably more sensitive to increased soil exposure than the shorter SWIR bands. As previously noted, the value in use of the SPOT data may be the higher spatial resolution, allowing for better discrimination of the burn boundaries.

The magnitudes of the SPOT data are slightly higher than Landsat for both NIR and SWIR bands. This may be due to the higher spatial resolution of SWIR and influence of soil. Because SPOT pixels have smaller spatial resolution they may be more sensitive to the reflection of bareground, thus their values are higher. Higher SPOT values may be also the result of the sensors' calibration. Most importantly, the SPOT results indicate that spectrally, it is less sensitive to post-fire effects such as burn severity than Landsat.

Our fire took place in the fall when vegetation was already senesced. Though it was proper to have imagery close to the fire dates, reflectance (and changes in reflectance) values were not as high as if the fire occurred in a spring or mid-summer fire. For example, because the SPOT SWIR (1.66μm) is sensitive to canopy moisture content, the band did not represent as much change because vegetation was dry in both pre-fire and post-fire images. Perhaps a study with an earlier fire date would show more definite results with the burn severity indices that used the SWIR (1.66μm) band.

An unknown level of bias was introduced in the field measure of burn severity because it was qualitative. A quantitative measure of burn severity would provide a more precise and accurate field assessment and enable comparison across multiple studies. Such an assessment needs to be established for rangeland application that is easy to learn and quick to perform in the field. Other possible errors include the timing of field sampling. Due to phenological changes, it is possible that a plot's fuel load could be mis-labeled. The pre-fire sampling was spread out over approximately 6 weeks, starting the end of June through August 5th. Craddock and Forsling (1938) determined that grass and forb growth is largely completed by July 1st. However we did note growth in lupine (*Lupinus argenteus)* and in birds beak (*Cordylanthus ramosus)*. Therefore, vegetation cover was slightly greater toward the end of the sampling season. However, this would only affect the results of the second hypothesis. Likewise, after the fire, grass established quickly. There was never more than 5% grass cover in a plot, but new cover was noted. It is important to note,

however, that the burn severity attribute and remote sensing indices were not affected by pre-fire sampling time because the pre-fire data were not used in those analyses.

Georegistration errors between the imagery and field data may be another source of error. An RMS error less than ½ a pixel is not much of a shift, but may be just enough to produce errors in the error matrix. Furthermore, (for hypothesis #2) during the post-fire surveys, we attempted to put plots in the same location using the GPS. Stakes were not used to delineate plot centers or boundaries due to regulations at the USSES. It was easier to have better accuracy with the point frame plots because we were able to lay out the perimeter based on a polygon shapefile in the GPS; however, the ocular estimates were located using only a point. Because of this, there is likely more georegistration error introduced in the ocular plots, which consisted of most of our field data. This would not affect the index results; it would only affect the results of the second hypothesis. Although a high precision GPS instrument was used (+/- 0.7m @ 95% CI) (Serr, unpublished) atmospheric effects may have also contributed to georegistration errors.

This study used 269 field plots for training and validation. Additional studies could be done to show the optimal number of training points for sufficient or better classification of burn severity.

The biggest limitation to our study is that the results are based on one burn and that it was a prescribed burn rather than natural. Because there were more than normal amounts of fine fuels (due to a wet spring) and because there were high winds during the fire, the majority of the burn was high burn severity. There was not a sufficient number of post-fire field plots in the low burn severity class to justify

having more categories, such as unburned, low, moderate, and high burn severity classes for classification. The few low burn severity plots were incorporated into the moderate burn severity class and considered 'incompletely burned' because the sample size was too low to have its own class. Inclusion of the low burn severity data in the moderate class may have skewed the data resulting in misrepresented moderate severity data. One possibility would have been to discard the low severity data all together. It would be useful to develop a burn severity classification with more detailed categories such as unburned, low, moderate, and high. Because there were not enough unburned and low burn severity plots within the burn perimeter, the hypothesis #2 sub-study (which correlated pre-fire fuel loads with burn severity) could only be performed between the moderate and high burn severity plots.

Hyperspectral imagery should be further explored to detect burn severity in rangelands because it may have wavelengths and corresponding bandwidths that are more sensitive to fire effects. For instance, AVIRIS channels 60 and 148, as suggested by van Wagtendonk et al. (2004), may discriminate fire effects better than Landsat bands 4 and 7 in rangelands. Another area for further study is performing an extended assessment of burn severity (the spring following the burn). It may be possible that rangeland burn severity is best detected with an extended assessment. An extended assessment may delineate areas of high burn severity better, either where perennial vegetation has not recovered or where introduced annuals have established.

The best burn severity index using SPOT imagery was the SAVI index (Fig. 10). However, our results with SAVI are contradictory with Epting's et al. (2005)

results whereas their SAVI and MSAVI indices performed worse than their indices incorporating mid-infrared bands. Their study area is in a coastal, cloudy region (Alaska) with potentially more atmospheric haze making the red band ineffective. More importantly, their study area was in a forested ecosystem. As suggested by White et al. (1996), Epting et al. (2005), and Roy et al. (2006) different burn severity indices may be needed across different ecosystem types. Furthermore, if better burn severity accuracies (>76% users and >63% producer's) are needed for recovery purposes within high burn severity areas, then a different algorithm should be sought.

The remote sensing indices used in this study are reproducible and straightforward. We chose to focus on remote sensing methods that incorporate satellite imagery and fit the needs of land managers (reasonable cost and practical spatial and spectral resolution) and methods that would not require the user to incorporate *large* amounts of field studies. This, after all, is the intent of remotely sensed models. The spatial resolution of imagery is ultimately determined by the necessary scale of fire recovery efforts. Because fire recovery efforts vary according to remoteness, economic impacts of the burn, and burn severity, land managers may require different types of satellite imagery. Though our best results are with the burned versus unburned algorithms, a 73% overall accuracy for the RdNBR burn severity index encourages future research. The RdNBR provided the best initial assessment users and producer's accuracies for this rangeland prescribed burn indicating its usefulness to land managers. These accuracies show moderate agreement between the index burn severity classes and the field-based burn severity classes. Before this index is entirely recommended, however, more studies need to be

performed using the RdNBR in rangelands that have heterogeneous fuel loads, and within burns that have variable burn severities. Future research entailing an extended assessment and the application of hyperspectral imagery is necessary to contribute to our understanding of burn severity in rangeland ecosystems and vegetation recovery.

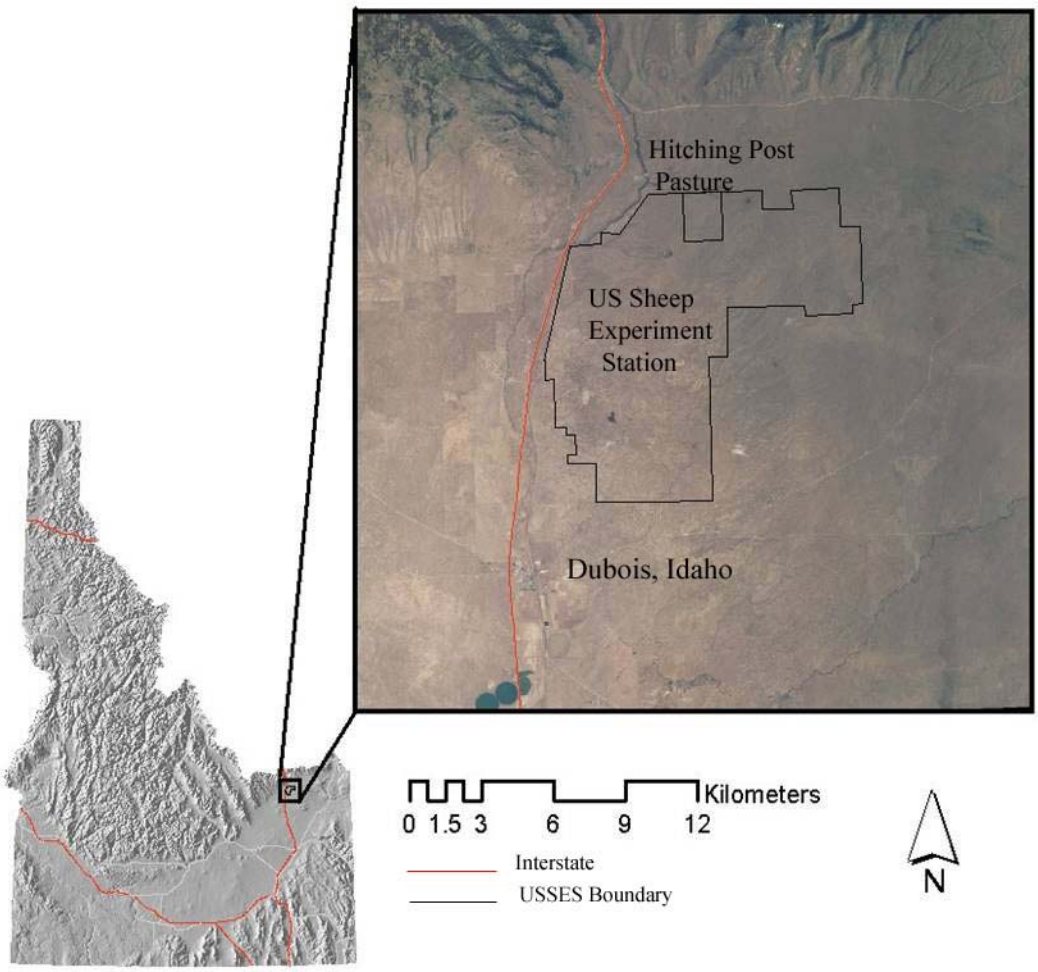

Figure 1. Location of the Hitching Post pasture study area in southeastern Idaho.

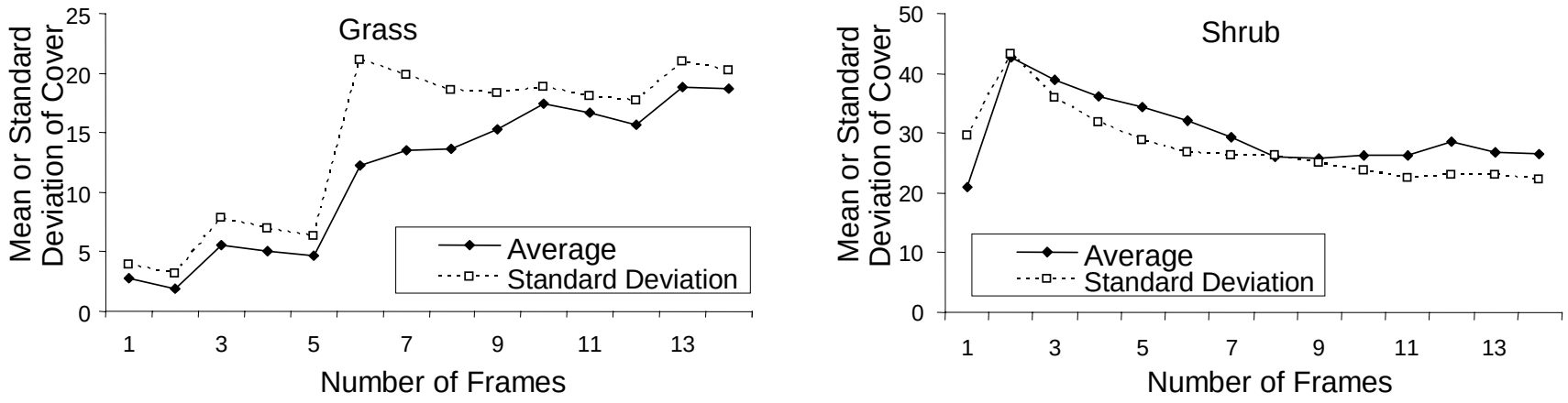

Figure 2. A sample effort curve is used to determine the necessary sampling intensity from one 20 x 40 m plot. Above, the cumulated mean (boxes) and standard deviation (diamonds) of shrub and grass cover for the plot level out around ten, indicating the need for approximately ten frames to estimate shrub and grass cover.

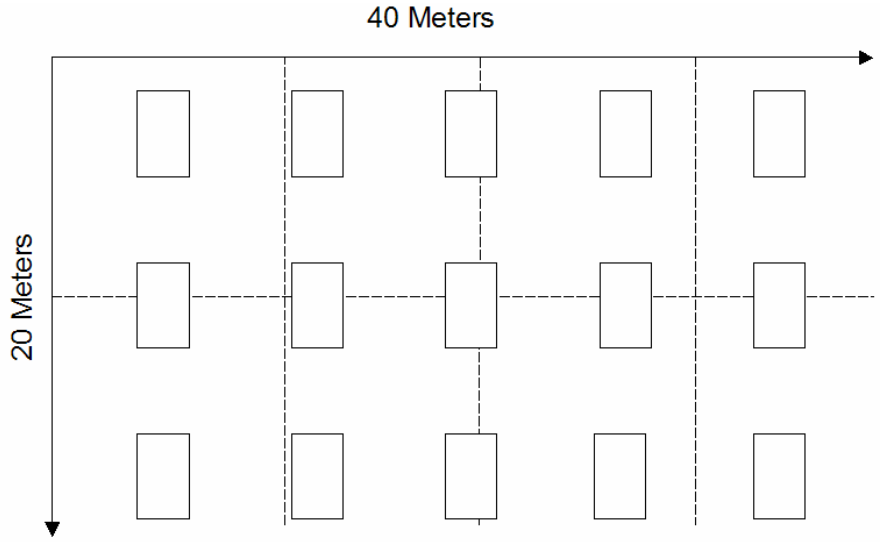

Figure 3. Approximate location of 15 point frames within each 20 x 40 m plot. Dashed lines indicate potential SPOT pixel 10 x 10 m placement.

Figure 4. Pre- and post-fire sampling plot locations, prescribed fire boundaries, and bulldozer-created fireline.

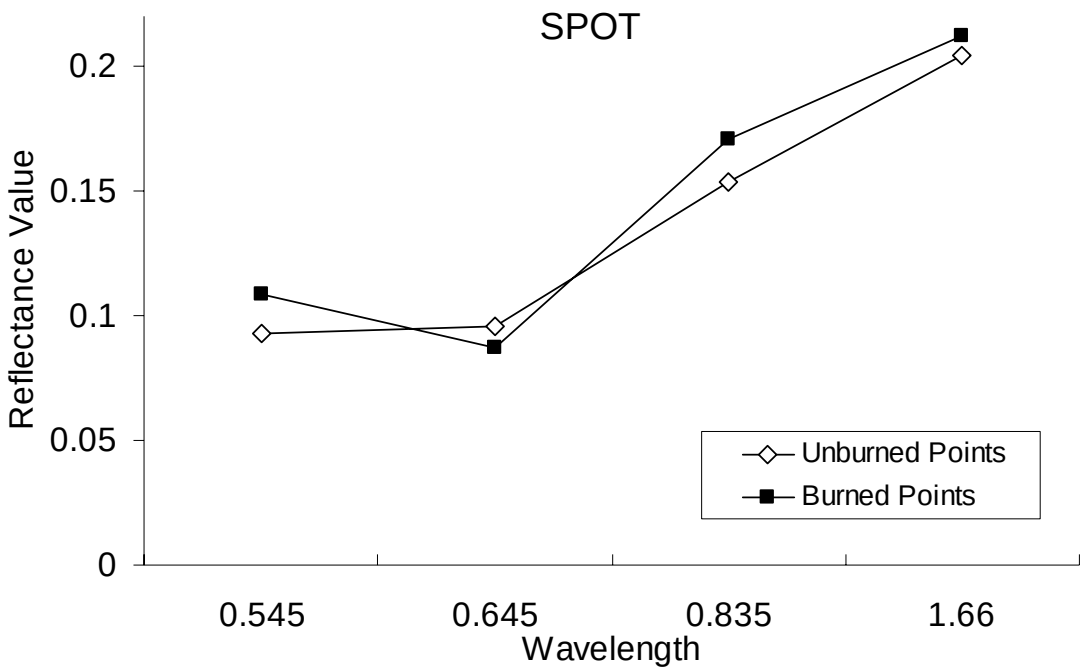

Figure 5. Pre-fire and post-fire SPOT imagery is used to demonstrate homogenous point frame plot (n = 36) reflectance averages.

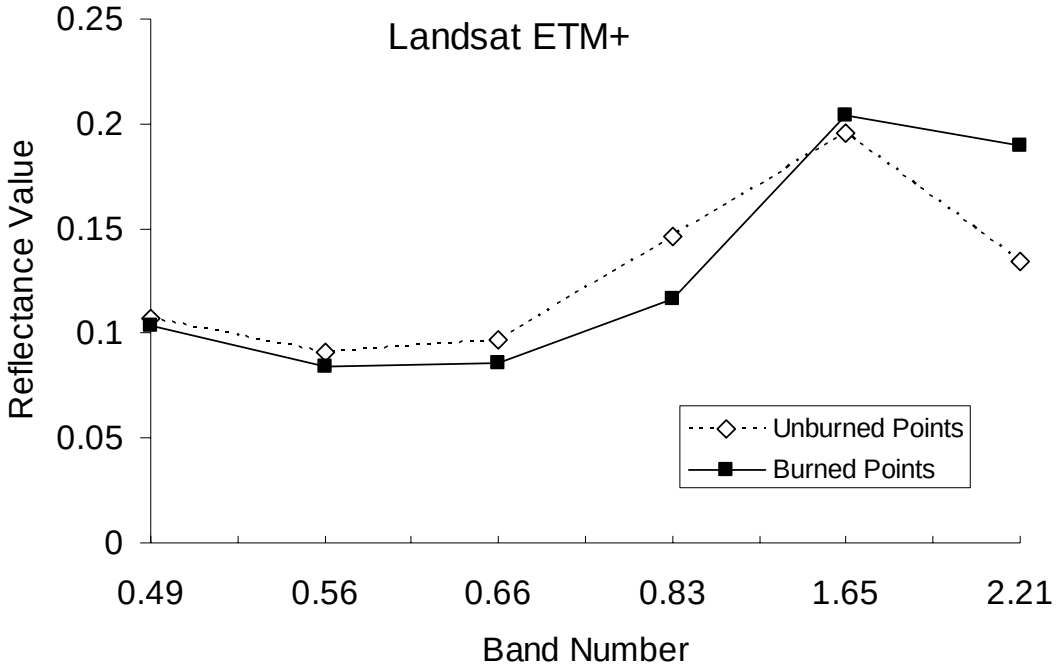

Figure 6. Pre-fire and post-fire Landsat imagery is used to demonstrate homogenous point frame plot (n=32) reflectance averages.

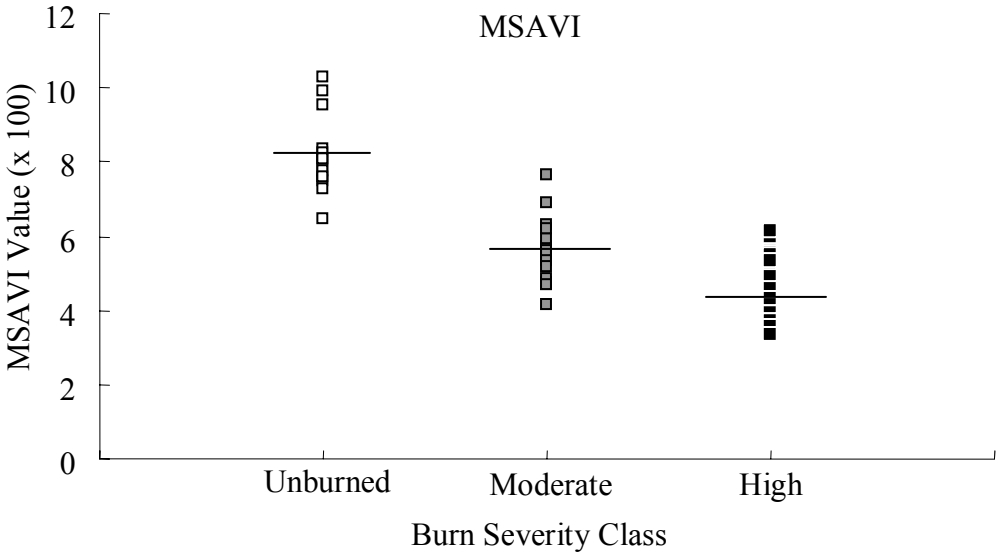

Figure 7. Example of a categorical scatterplot of burn severity classes versus the Landsat MSAVI index. Dashes indicate mean index values of the burn severity class.

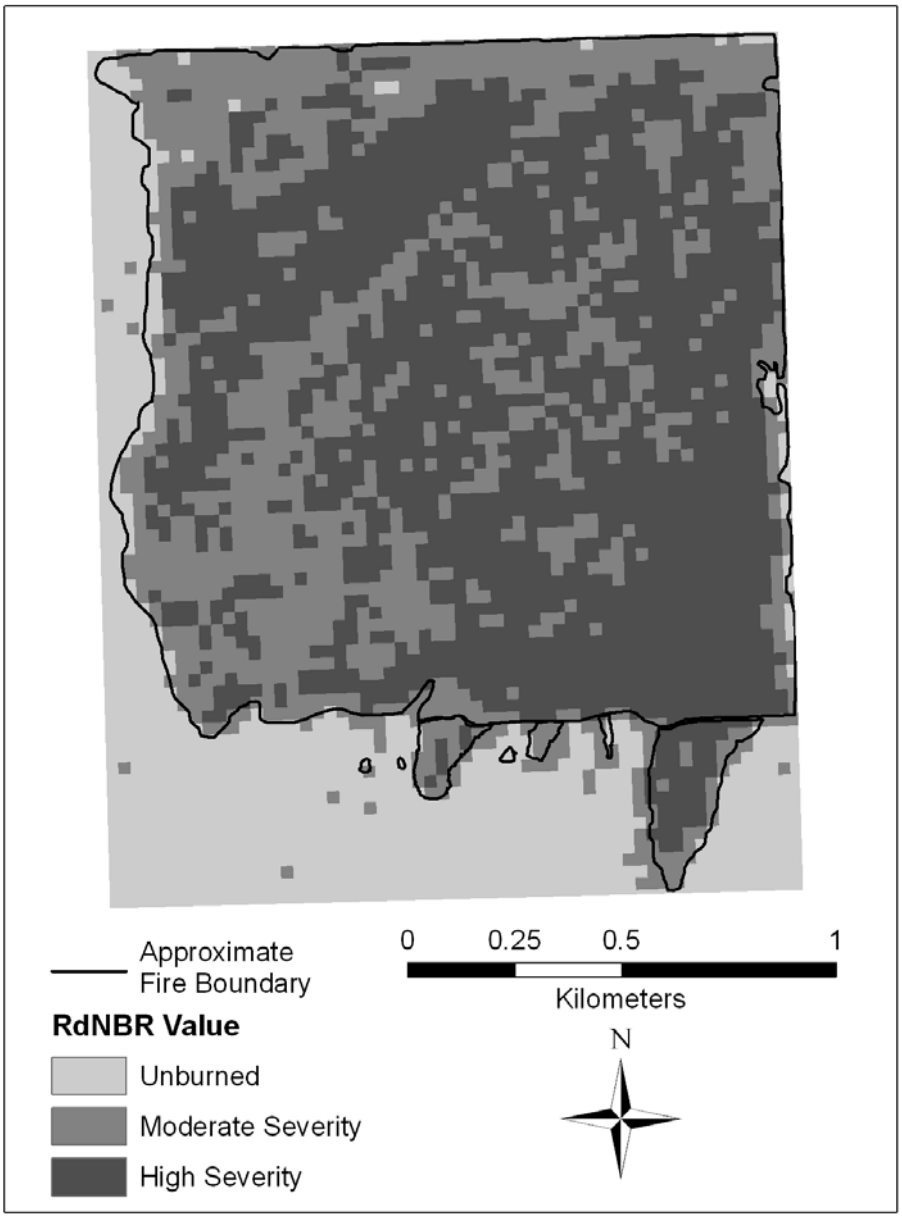

Figure 8. The relative differenced NBR using Landsat data.

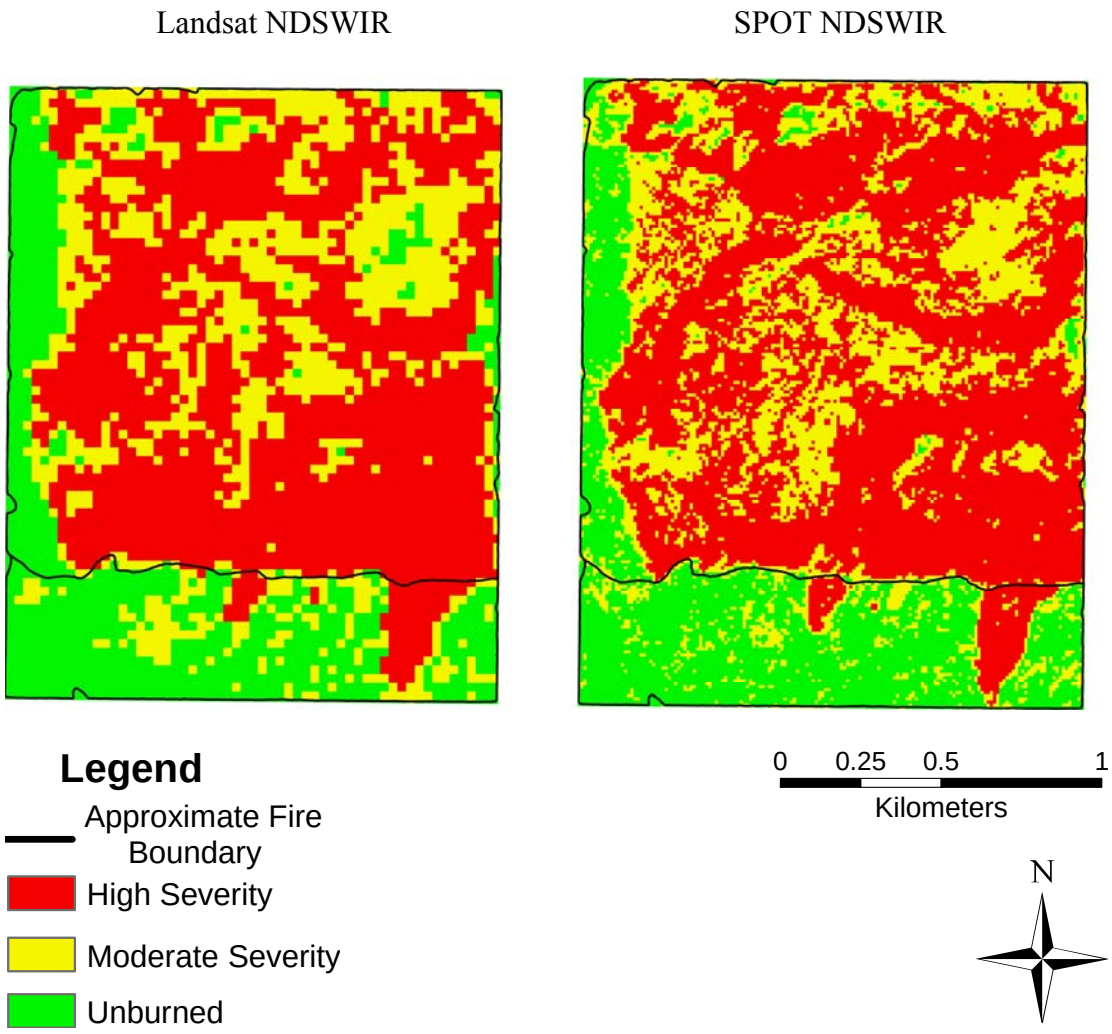

Figure 9. Comparison of the burn severity Landsat and SPOT NDSWIR results.

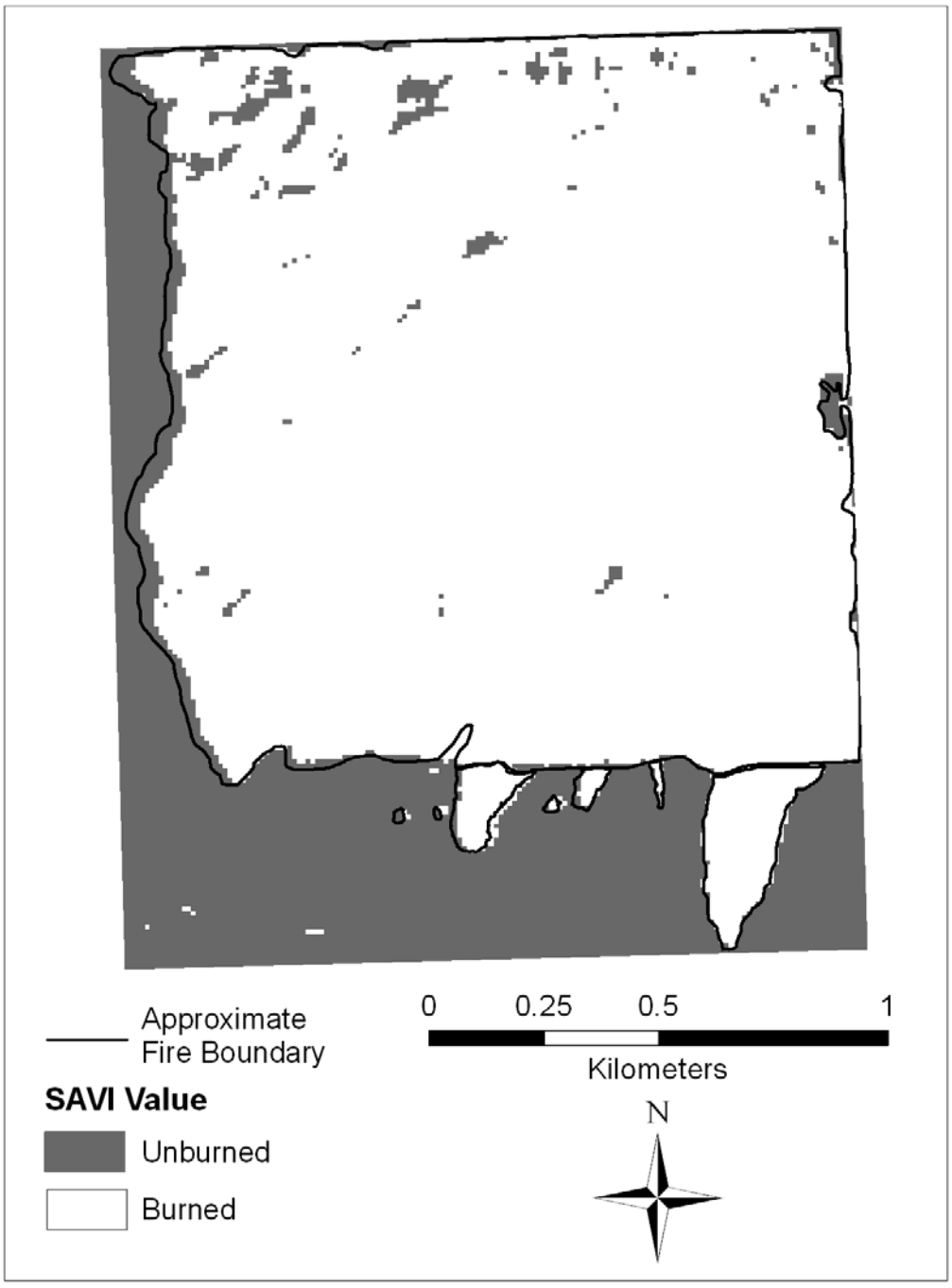

Figure 10. The SAVI burned versus unburned index using SPOT data.

Table 1. Remote sensing indices that were explored to find the best burn/no burn algorithm and the best burn severity algorithm.

Remote Sensing Index	Algorithm	Sensor	References
SAVI	$\frac{(1+L)(NIR-Red)}{NIR+Red+L}$ (L = 0.5)	Landsat: NIR = band 4 Red = band 3 SPOT: NIR = band 3 Red = band 2	Huete, 1988
MSAVI	$\frac{2*(NIR)+1-\sqrt{(2*(NIR)+1)2-8*(NIR-Red)}}{2}$	Landsat: NIR = band 4 Red = band 3 SPOT: NIR = band 3 Red = band 2	Qi et al., 1994
pNDSWIR	$\frac{NIR-SWIR}{NIR+SWIR}$	Landsat: NIR = band 4 SWIR = band 5	
NDSWIR	Pre-fire NDSWIR – Post-fire NDSWIR	SPOT: NIR = band 3 SWIR = band 4	Gerard et al., 2003
NBR	$\frac{NIR-SWIR}{NIR+SWIR}$	Landsat: NIR = band 4 SWIR = Band 7	Lopez Garcia and Caselles, 1991; Key and Benson, 1999b; 2004a
dNBR	Pre-fire NBR –Post-fire NBR		
RdNBR	$\frac{Pre\text{-}fireNBR-Post\text{-}fireNBR}{\sqrt{prefireNBR}}$	Landsat: NIR = band 4 SWIR = band 7	Miller and Thode, in revision
Modified NDVI	$\frac{SWIR-Red}{SWIR+Red}$	SPOT: Red = band 2 SWIR = band 4	None
rModNDVI	$\frac{Pre\text{-}fireModNDVI-Post\text{-}fireModNDVI}{\sqrt{Pre\text{-}fireModNDVI}}$		

Table 2. Categorical groups of percent cover.

Percent Cover	Cover Class
None	0
1-5%	1
6-15%	2
15-25%	3
26-35%	4
36-50%	5
51-75%	6
>75%	7

Table 3. Field attributes for all ocular estimates collected with an ArcPad customized form within a Trimble GeoXT GPS receiver.

Attributes
Plot ID and its center point location
Date
Percent cover of: dominant shrub
Percent cover of: other shrubs present
Average shrub height (Low: <51cm, Medium: 51-100cm, Tall: >100cm)
Percent cover of: grass
Percent cover of: litter
Percent cover of: bareground
Percent cover of: rock
Percent cover of: forb
Percent cover of: dominant weed
Fuel load (Low: Grass only, Medium: small to medium sized shrubs, High: tall, dense shrubs)
Sage diameter measured once in each cardinal direction
Photos taken in 4 cardinal directions & their ID #
Presence of microbiotic crust
Observed vegetation type (GAP classification category which was 'Sagebrush Grassland', defined by the Idaho GAP 2 data set (2000),
Litter type (oxidized gray or biologically brown)
Plot homogeneity (as described in Field Methods)

Table 4. Point frame plot field attributes collected with Trimble GeoXT GPS receiver and ArcPad customized form.

Attributes
Plot ID and its boundary location
Fuel load (3 categories) or Burn Severity
Plot homogeneity (as described in Field Methods)

Table 5. Description of burn severity categories based on an ocular estimate.

Burn Severity Value	Category	Definition
Unburned	1	Vegetation is in same condition as pre-fire
Moderate	2	Vegetation was burned within the plot
High	3	100% vegetation was burned within plot

Table 6. Dates and location of SPOT and Landsat imagery.

Imagery	Date	Scene ID/Path Row
SPOT 5 Pre-fire	27-Aug-05	547-260
SPOT 5 Post-fire	28-Sep-05	547-260
Landsat ETM+ Pre-fire	4-Jul-05	39/29
Landsat ETM+ Post-fire	24-Oct-05	39/29

Table 7. Root Mean Square Error (RMSE) of the Landsat and SPOT data.

Imagery	RMSE	Distance off (m)
Landsat	0.2621	7.9
SPOT	0.3489	3.5

Table 8. Number of training plots and validation plots when assessing all remote sensing indices.

Burn Severity Value	Category	# of Training Plots	# of Validation Plots
Unburned	1	14	50
Moderate	2	16	50
High	3	89	50

Table 9. An example of an error matrix table with Kappa results: the Landsat relative dNBR burn severity index.

	Unburned	Moderate	High	Total
Unburned	43	1	0	44
Moderate	6	28	12	46
High	1	21	38	60
Total	50	50	50	150
Overall Accuracy	73%			
Users Accuracy	86%	56%	76%	
Producer's Accuracy	98%	61%	63%	
KHAT	0.49			
Variance	0.0033			
Z Statistic	8.4339			

Table 10. 'Burned versus unburned' remote sensing index accuracies and kappa statistics using SPOT 5 imagery.

Accuracy Type	dNDSWIR	pNDSWIR	RelModNDVI	MSAVI	SAVI
Overall Accuracy	65%	96%	94%	95%	100%
Producer's Unburned	49%	96%	94%	98%	100%
Users Unburned	82%	92%	88%	86%	100%
Producer's Burned	86%	96%	94%	93%	100%
Users Burned	57%	98%	97%	99%	100%
KHAT	0.3333	0.9091	0.862944	0.8763	1.0000
Variance	0.0068	0.0013	0.001955	0.0017	0.0000
Z Stat	4.0239	25.0211	19.51918	20.6704	*

Table 11. An example of an error matrix table: the SPOT SAVI index with 100% overall accuracy.

		Reference Data		
		Unburned	Burned	Total
Remote	Unburned	50	0	50
Sensing	Burned	0	100	100
Data	Total	50	100	150
	Overall			100%
	Users	100%	100%	
	Producers	100%	100%	

Table 12. 'Burned versus unburned' remote sensing index accuracies and kappa statistics using Landsat ETM+ imagery.

Accuracy Type	dNBR	RdNBR	NDSWIR	MSAVI	SAVI
Overall Accuracy	94%	95%	89%	95%	95%
Producer's Unburned	96%	98%	90%	94%	94%
Users Unburned	86%	86%	74%	90%	90%
Producer's Burned	93%	93%	88%	95%	95%
Users Burned	98%	99%	96%	97%	97%
KHAT	0.8615	0.8763	0.7329	0.8788	0.8787
Variance	0.0019	0.0018	0.0036	0.0017	0.0017
Z Stat	19.3140	20.6704	12.1327	21.1018	21.1017

Table 13. 'Burn severity' remote sensing index accuracies and kappa statistics using Landsat ETM+ imagery.

Accuracy Type	dNBR	RdNBR	NDSWIR	MSAVI	SAVI
Overall Accuracy	66%	73%	58%	66%	67%
Producer's Unburned	96%	98%	90%	94%	94%
Producer's Moderate	50%	61%	37%	50%	52%
Producer's High	55%	63%	52%	55%	57%
Users Unburned	86%	86%	74%	90%	90%
Users Moderate	38%	56%	34%	42%	44%
Users High	74%	76%	66%	66%	68%
KHAT	0.4900	0.5900	0.37000	0.4900	0.5100
Variance	0.0033	0.0030	0.00375	0.0034	0.0033
Z Stat	8.4339	10.7668	6.04186	8.4456	8.8829

Table 14. 'Burn severity' remote sensing index accuracies and kappa statistics using SPOT 5 imagery.

Accuracy Type	dNDSWIR	rModNDVI	pNDSWIR	MSAVI	SAVI
Overall Accuracy	65%	67%	69%	67%	71%
Producer's Unburned	95%	94%	96%	98%	100%
Producer's Moderate	49%	58%	56%	51%	61%
Producer's High	56%	54%	58%	55%	55%
Users Unburned	82%	88%	92%	86%	100%
Users Moderate	40%	28%	40%	38%	38%
User's High	74%	86%	76%	76%	76%
KHAT	0.4800	0.5100	0.5400	0.5000	0.5700
Variance	0.0034	0.003223	0.0032	0.0033	0.0030
Z Stat	0.0819	8.983351	9.6167	8.6376	10.391

REFERENCES

Anderson, H.E. (1982). Aids to determining fuel models for estimating fire behavior. General Technical Report INT-122. Intermountain Forest and Range Experiment Station Ogden, UT.

Anderson, J.E. and Inouye, R.S. (2001). Landscape-scale changes in plant species abundance and biodiversity of a sagebrush steppe over 45 years. *Ecological Monographs,* 71, 531-556

Asner, G.P. (2004). Biophysical remote sensing signatures of arid and semiarid ecosystems. Remote Sensing for Natural Resource Management and Environmental Monitoring. 3 ed., ed S. L. Ustin, 53-109. Vol. 4. Hoboken, New Jersey: John Wiley and Sons.

Asner, G.P. and Heidebrecht, K.B. (2002). Spectral unmixing of vegetation, soil and dry carbon cover in arid regions: comparing multispectral and hyperspectral observations. *International Journal of Remote Sensing*, 23:19, 3939-3958

Bannari, A., Morin, D., Bonn, F., and Huete, A.R. (1995). A review of vegetation indices. *Remote Sensing Reviews,* 13, 95-120

Brewer, C.K., Winne, J.C., Redmond, R.L., Opitz, D.W., and Mangrich, M.V. (2005). Classifying and mapping wildfire severity: A comparison of methods. *Photogrammetric Engineering and Remote Sensing,* 71:11, 1311-20

Brown, James K.; Smith, Jane Kapler, eds. 2000. Wildland fire in ecosystems: effects of fire on flora. Gen. Tech. Rep. RMRS-GTR-42-vol. 2. Ogden, UT: U.S. Department of Agriculture, Forest Service, Rocky Mountain Research Station. 257 p. URL: http://www.fs.fed.us/rm/pubs/rmrs_gtr42_2.pdf; Last accessed July 28, 2006.

Cocke, A.E., Fule, P.Z., and Crouse, J.E. (2005). Comparison of burn severity assessments using differenced normalized burn ratio and ground data. *International Journal of Wildland Fire,* 14, 189-98

Congalton, R. and Green, K. (1999). Assessing the accuracy of remotely sensed data: principles and practices. (pp. 137). Washington, D.C.: CRC Press, Inc.

Craddock, G.W. and Forsling, C.L. (1938). The influence of climate and grazing on spring-fall sheep range in southern Idaho. United States Department of Agriculture Technical Bulletin No. 600. URL: http://warp.nalusda.gov/ref/USDApubs/tb.htm#sortnbr; Last accessed September 28, 2006.

Diaz-Delgado, R., Lloret, F., Pons, X., and Terradas, J. (2002). Satellite evidence of decreasing resilience in mediterranean plant communities after recurrent

wildfires. *Ecology,* 83, 2293-2303

Diaz-Delgado, R., Lloret, F., and Pons, X. (2003). Influence of fire severity on plant regeneration by means of remote sensing imagery. *International Journal of Remote Sensing*, 24:8, 1751-1763

Epting, J. and Verbyla, D. (2005). Landscape-level interactions of pre-fire vegetation, burn severity, and post-fire vegetation over a 16-year period in interior Alaska. *Canadian Journal of Forest Research*, 35:6, 1367-1377

Epting, J., Verbyla, D., and Sorbel, B. (2005). Evaluation of remotely sensed indices for assessing burn severity in interior alaska using Landsat TM and ETM+. *Remote Sensing of Environment*, 96, 328-339

Flasse, S., Trigg, S., Ceccato, P., Perryman, A., Hudak, A., Thompson, M., Brockett, B., Dramé, M., Ntabeni, T., Frost, P., Landmann, T., and le Roux, J. (2004). Remote sensing of vegetation fires and its contribution to a fire management information system. In J.G. Goldammer and C. de Ronde (Ed.), *Wildfire Management Handbook for Sub-Sahara Africa* (pp.158-211). The Hague, Netherlands: SPB Publishing

Floyd, D.A. and Anderson, J.E. (1982). A new point interception frame for estimating cover of vegetation. *Vegetatio,* 50, 185-186

Floyd, D.A. and Anderson, J.E. (1987). A comparison of three methods for estimating plant cover. *Journal of Ecology,* 75, 221-228

Garcia, M. and Chuvieco, E. (2004). Assessment of the potential of SAC-C/MMRS imagery for mapping burned areas in Spain. *Remote Sensing of Environment,* 92, 414-423

Gerard, F., Plummer, S., Wadsworth, R., Ferreruela Sanfeliu, A., Iliffe, L., Balzter, H., and Wyatt, B. (2003). Forest fire scar detection in the boreal forest with multi-temporal SPOT-VEGETATION data. *Geoscience and Remote Sensing, IEEE Transactions on,* 41:11, 2575-2585

GIS Training and Research Center (TReC). (2006). URL: http://giscenter.isu.edu/software/index.htm Last accessed: October 16, 2006

Harniss, R.O. and Murray, R.B. (1973). 30 Years of Vegetal Change Following Burning of Sagebrush-Grass Range. *Journal of Range Management*, 26, 322-325

Howard, S.M. and Lacasse, J.M. (2004). An evaluation of gap-filled Landsat SLC-Off imagery for wildland fire burn severity mapping. *Photogrammetric Engineering and Remote Sensing*, 701:8, 877-880

Huete, A.R., Jackson, R.D., and Post, D.F. (1987) Spectral response of a plant canopy

with different soil backgrounds. *Remote Sensing of Environment,* 17:11, 37-54

Huete, A.R. (1988). A soil-adjusted vegetation index (SAVI). *Remote Sensing of Environment,* 25, 295-309

Huete, A.R. (1989). Soil influences in remotely sensed vegetation-canopy spectra. In G. Astrar (Ed.), *Theory and Applications of Optical Remote Sensing* (pp.107-41). New York: Wiley, Wiley

Inouye, R.S. (2002). Sampling effort and vegetative cover estimates in sagebrush steppe. *Western North American Naturalist*, 62, 360-364

Jensen, J.R. (1996). *Introductory Digital Image Processing: A Remote Sensing Perspective*. (pp. 318). New Jersey, USA: Prentice-Hall, Inc.

Jensen, J.R. (2000). *Remote Sensing of the Environment: An Earth Resource Perspective.* (pp. 544). New Jersey, USA: Prentice-Hall, Inc.

Keeley, J.E., Fotheringham, C.J., and Morais, M. (1999). Reexamining fire suppression impacts on brushland fire regimes. *Science,* 284, 1829-1832

Key, C.H. and Benson, N.C. (1999a). The Composite Burn Index (CBI): Field Rating of Burn Severity. URL: http://www.nrmsc.usgs.gov/research/cbi.htm;Last accessed July 28, 2006

Key, C.H. and Benson, N.C. (1999b). The Normalized Burn Ratio (NBR): A Landsat TM Radiometric Index of Burn Severity. URL: http://www.nrmsc.usgs.gov/research/ndbr.htm; Last accessed July 28, 2006

Key, C.H. and Benson, N.C. (2004a). Remote Sensing Measure of Severity: The Normalized Burn Ratio. FIREMON Landscape Assessment (LA) V4 Sampling and Analysis Methods. pp. LA1-16

Key, C.H. and Benson, N.C. (2004b). Ground Measure of Severity: The Composite Burn Index. FIREMON Landscape Assessment (LA) V4 Sampling and Analysis Methods pp. LA_CBI_Plot-1-9

Key, C.H. and Benson, N.C. (2006). Landscape Assessment (LA) Sampling and Analysis Methods. USDA Forest Service Gen. Tech. Rep. RMRS-GTR-164-CD. pp. 55

Lillesand, T.M., Kiefer, R.W., and Chipman, J.W. (2004). *Remote Sensing and Image Interpretation.* (pp. 1-500). New York: Wiley

Lopez Garcia, M.J. and Caselles, V. (1991). Mapping burns and natural reforestation using thematic mapper data. *Geocarto International,* 6, 31-37

Lutes, D.C., Keane, R.E., Caratti, J.F., Key, C.H., Benson, N.C., Sutherland, S., and

Gangi, L.J. (2003). FIREMON: Fire Effects Monitoring and Inventory System, Extended abstract submitted to: American Meteorological Society 2nd International Wildland Fire Ecology and Fire Management Congress, November 2003, Orlando, FL. URL:http://ams.confex.com/ams/pdfpapers/65637.pdf Last accessed October 16, 2006

McGwire, K., Minor, T., and Fenstermaker, L. (2000). Hyperspectral mixture modeling for quantifying sparse vegetation cover in arid environments. *Remote Sensing of Environment,* 72, 360-374

McMahan, J.B., Narsavage, D., and Weber, K. (2003). The "Pole Cam": corroborating field estimations with high spatial resolution imagery. In K. Weber (Ed.), *Final Report: Wildfire Effects on Rangeland Ecosystems and Livestock Grazing in Idaho* (pp. 18-22). Idaho State University URL: http://giscenter.isu.edu/research/techpg/nasa_wildfire/template.htm Last accessed October 16, 2006

Miller, J.D. and Thode, A.E. (in revision). Quantifying burn severity in a heterogeneous landscape with a relative version of the delta Normalized Burn Ratio (dNBR). *Remote Sensing of Environment*

Miller, J.D. and Yool, S.R. (2002). Mapping forest post-fire canopy consumption in several overstory types using multi-temporal Landsat TM and ETM data. *Remote Sensing of Environment,* 82, 481-96

Miller, R.F. and Rose, J.A. (1999). Fire history and western juniper encroachment in sage-brush steppe. *Journal of Range Management,* 52, 550-559

Morgan, P., Hardy, C.C., Swetnam, T.W., Rollins, M.G., and Long, D.G. (2001). Mapping fire regimes across time and space: Understanding coarse and fine-scale fire patterns. *International Journal of Wildland Fire,* 10, 329–342

National Interagency Fire Center (NIFC). (2006). Wildland Fire Statistics. URL: http://www.nifc.gov/stats/fires_acres.html; Last accessed September 26, 2006

Natural Resources Conservation Service (NRCS). (1995). Soil investigation of Agriculture Research Service, United States Sheep Experiment Station headquarters range, US Department of Agriculture. (pp. 133). Rexburg, ID: NRCS

Obrist, D., Delucia, E.H., and Arnone, J.A. (2003). Consequences of wildfire on ecosystem CO2 and water vapour fluxes in the Great Basin. *Global Change Biology*, 9, 563-74

Okin, G.S., Roberts, D.A., Murray, B., and Okin, W.J. (2001). Practical limits on hyperspectral vegetation discrimination in arid and semiarid environments.

Remote Sensing of Environment, 77, 212-225

Patterson, M.W. and Yool, S.R. (1998). Mapping fire-induced vegetation mortality using Landsat Thematic Mapper data: A comparison of linear transformation techniques. *Remote Sensing of Environment*, 65, 132-42

Perryman, B.L. and Olson, R.A. (2000). Age-stem diameter relationships of big sagebrush and their management implications. *Journal of Range Management*, 53, 342-346

Qi, J., Chehbouni, A., Heute, A.R., Kerr, Y.H., and Sorooshian, S. (1994). A modified soil adjusted vegetation index. *Remote Sensing of Environment,* 48, 119-126

Rahman, A. and Gamon, J. (2004). Detecting biophysical properties of a semi-arid grassland and distinguishing burned from unburned areas with hyperspectral reflectance *Journal of Arid Environments,* 58, 597-610

Ratzlaff, T.D. and Anderson, J.E. (1995). Vegetal recovery following wildfire in seeded and unseeded sagebrush steppe. *Journal of Range Management*, 48, 386-391

Rouse, J.W., Haas, R.H., Schell, J.A., and Deering, D.W. (1973). Monitoring vegetation systems in the great plains with ERTS'. Third ERTS Symposium, NASA SP-351 I, 309-317

Roy, D.P., Boschetti, L., and Trigg, S.N. (2006). Remote sensing of fire severity: Assessing the performance of the normalized burn ratio. *IEEE Geoscience and Remote Sensing Letters*, 3, 112-116

RSI. (2005). *ENVI user's guide (Version 4.2)*. Research Systems Incorporated (pp. 1201). Boulder, Colorado

Ruiz-Gallardo, J.R., Castańo, S., and Calera, A. (2004). Application of remote sensing and GIS to locate priority intervention areas after wildland fires in Mediterranean systems: a case study from south-eastern Spain. *International Journal of Wildland Fire*, 13, 241-252

Russell, G. and Weber, K. (2003). Field collection of fuel load, vegetation characteristics, and forage measurements on rangelands of the upper Snake River Plain, ID for wildfire fuel and risk assessment models. In K. Weber (Ed.), *Final Report: Wildfire Effects on Rangeland Ecosystems and Livestock Grazing in Idaho* (pp. 4-11). Idaho State University URL: http://giscenter.isu.edu/research/techpg/nasa_wildfire/template.htm Last accessed October 16, 2006

Ryan, K.C. and Noste, N.V. (1983). Evaluating prescribed fires. In: J.E. Lotan, B.M.

Kilgore, W.C. Fischer, and R.W. Mutch, Tec. Coord. Proc. Symposium and Workshop on Wilderness Fire. USDA Forest Service General Tec. Rep. INT-182. Intermountain Forest and Range experiment Station, Ogden, UT. 230-238

Salvador, R., Valeriano, J., Pons, X., and Diaz-Delgado, R. (2000). A semi-automatic methodology to detect fire scars in shrubs and evergreen forests with Landsat MSS time series. *International Journal of Remote Sensing,* 21, 655-71

Sannier, C. (1999). Strategic monitoring of crop yields and rangeland conditions in southern Africa with remote sensing. PhD Thesis, Cranfield University: Silsoe College

Santos, T.G., Caetano, M.R., Barbosa, P.M., and Paúl, J.U. (1999). A comparative study of vegetation indices to assess land cover change after forest fires. *Remote Sensing for Earth Science, Ocean, and Sea Ice Applications*, 3868, 232-240

Schmidt, H. and Karnieli, A. (2001). Sensitivity of vegetation indices to substrate brightness in hyper-arid environment: the Makhtesh Ramon Crater (Israel) case study. *International Journal of Remote Sensing,* 22, 3503-3520

Schowengerdt, R.A. (1997). *Remote Sensing: Models and Methods for Image Processing*. (pp. 182-355). San Diego: Academic Press

Seefeldt, S.S. (2005). Consequences of selecting rambouilllet ewes for mountain big sagebrush (Artemisia tridentata ssp. vaseyana) dietary preference. *Rangeland Ecology and Management,* 58, 380-384

Smith, A.M.S., Wooster, M.J., Drake, N.A., Dipotso, F.M., Falkowski, M.J., and Hudak, A.T. (2005). Testing the potential of multi-spectral remote sensing for retrospectively estimating fire severity in African savannahs. *Remote Sensing of Environment*, 97, 92-115

Turner, M.G., Hargrove, W.W., Gardner, R.H., and Romme, W.H. (1994). Effects of fire on landscape heterogeneity in Yellowstone National Park, Wyoming. *Journal of Vegetation Science*, 5, 731-42

USDA Forest Service. (2001). Field measurements for the training and validation of burn severity maps from spaceborne, remotely sensed imagery. Remote Sensing Applications Center, Salt Lake City, (UT): USDA Forest Service, Final Project Report, Joint Fire Science Program-2001-2. Project # 01B-2-1-01, pp. 15 URL: http://www.fs.fed.us/eng/rsac/baer/jfs.html Last accessed October 15, 2006

USDI National Park Service. (2003). Fire monitoring handbook. Boise, (ID): Fire Management Program Center, National Interagency Fire Center. pp. 274

van Wagtendonk, J.W., Root, R.R., and Key, C.H. (2004). Comparison of AVIRIS and Landsat ETM+ detection capabilities for burn severity. *Remote Sensing of Environment,* 92, 397–408

Watts, M.J. and Wambolt, C.L. (1996). Long-term recovery of Wyoming big Sagebrush after four treatments. *Journal of Environmental Management*, 46, 95-102

Weber, K. and McMahan, J.B. (2003). Field collection of fuel load and vegetation characteristics wildfire risk assessment modeling: 2002 field sampling report. In K. Weber (Ed.), *Final Report: Wildfire Effects on Rangeland Ecosystems and Livestock Grazing in Idaho* (pp. 12-16). Idaho State University URL: http://giscenter.isu.edu/research/techpg/nasa_wildfire/template.htm Last accessed October 16, 2006

West, N.E. and Young, J.A. (2000). Intermountain Valleys and Lower Mountain Slopes. In M.G. Barbour and W.D. Billings (Ed.), *North American Terrestrial Vegetation* (pp. 255-284). Cambridge, UK: Cambridge University Press

Whisenant, S. (1990). Changing fire frequencies on Idaho's Snake River plains: Ecological and management implications. p. 4-10, in Proceedings from the Symposium on Cheatgrass Invasion, Shrub Dieoff, and Other Aspects of Shrub Biology and Management. U.S. Forest Service General Technical Report INT-276

White, J.D., Ryan, K.C., Key, C.C., and Running, S.W. (1996). Remote sensing of forest fire severity and vegetation recovery. *International Journal of Wildland Fire*, 6, 125-36

Whitford, W. (2002). *Ecology of Desert Systems*. (pp. 343). California: Academic Press

Wimberly, M.C. and Reilly, M.J. (in press). Assessment of fire severity and species diversity in the southern appalacians using Landsat TM and ETM+ imagery. *Remote Sensing of Environment* (in press).

Wright and Bailey. (1982). *Fire Ecology*. (pp.528). New York: Wiley

Appendix I: Results of 10 Remote Sensing Indices

Table 15. Results of all SPOT burned versus unburned remote sensing indices.

SAVI		Reference Data		
		Unburned	Burned	Total
Remote	Unburned	50	0	50
Sensing	Burned	0	100	100
Data	Total	50	100	150
	Overall	100%		
	Users	100%	100%	
	Producers	100%	100%	

pNDSWIR		Reference Data		
		Unburned	Burned	Total
Remote	Unburned	46	2	48
Sensing	Burned	4	98	102
Data	Total	50	100	150
	Overall	96%		
	Users	92%	98%	
	Producers	96%	96%	

RelMod		Reference Data		
NDVI		Unburned	Burned	Total
	Unburned	44	3	47
Remote	Burned	6	97	103
Sensing	Total	50	100	150
Data	Overall	94%		
	Users	88%	97%	
	Producers	94%	94%	

MSAVI		Reference Data		
		Unburned	Burned	Total
Remote	Unburned	45	3	48
Sensing	Burned	5	97	102
Data	Total	50	100	150
	Overall	95%		
	Users	86%	99%	
	Producers	98%	93%	

dNDSWIR		Reference Data		
		Unburned	Burned	Total
Remote	Unburned	41	43	84
Sensing	Burned	9	57	66
Data	Total	50	100	150
	Overall	65%		
	Users	82%	57%	
	Producers	49%	86%	

Table 16. Results of all Landsat burned versus unburned remote sensing indices.

dNBR		Reference Data		
		Unburned	Burned	Total
Remote	Unburned	43	2	45
Sensing	Burned	7	98	105
Data	Total	50	100	150
	Overall	94%		
	Users	86%	98%	
	Producers	96%	93%	

NDSWIR		Reference Data		
		Unburned	Burned	Total
Remote	Unburned	37	4	41
Sensing	Burned	13	96	109
Data	Total	50	100	150
	Overall	89%		
	Users	74%	96%	
	Producers	90%	88%	

MSAVI		Reference Data		
		Unburned	Burned	Total
Remote	Unburned	45	3	48
Sensing	Burned	5	97	102
Data	Total	50	100	150
	Overall	95%		
	Users	94%	95%	
	Producers	90%	97%	

RdNBR		Reference Data		
		Unburned	Burned	Total
Remote	Unburned	43	1	44
Sensing	Burned	7	99	106
Data	Total	50	100	150
	Overall	95%		
	Users	86%	99%	
	Producers	98%	93%	

SAVI		Reference Data		
		Unburned	Burned	Total
Remote	Unburned	45	3	48
Sensing	Burned	5	97	102
Data	Total	50	100	150
	Overall	95%		
	Users	90%	97%	
	Producers	94%	95%	

Table 17. Results of all SPOT burn severity remote sensing indices.

SAVI		Reference Data			
		Unburned	Moderate	High	Total
Remote	Unburned	50	0	0	50
Sensing	Moderate	0	19	12	31
Data	High	0	31	38	69
	Total	50	50	50	150
	Overall	71%			
	Users	100%	38%	76%	
	Producers	100%	61%	55%	

pNDSWIR		Reference Data			
		Unburned	Moderate	High	Total
Remote	Unburned	46	2	0	48
Sensing	Moderate	4	20	12	36
Data	High	0	28	38	66
	Total	50	50	50	150
	Overall	69%			
	Users	92%	40%	76%	
	Producers	96%	56%	58%	

RelMod		Reference Data			
NDVI		Unburned	Moderate	High	Total
	Unburned	44	3	0	47
Remote	Moderate	3	14	7	24
Sensing	High	3	33	43	79
Data	Total	50	50	50	150
	Overall	67%			
	Users	88%	28%	86%	
	Producers	94%	58%	54%	

MSAVI		Reference Data			
		Unburned	Moderate	High	Total
Remote	Unburned	45	3	0	48
Sensing	Moderate	4	21	17	42
Data	High	1	26	33	60
	Total	50	50	50	150
	Overall	67%			
	Users	86%	38%	76%	
	Producers	98%	51%	55%	

dNDSWIR		Reference Data			
		Unburned	Moderate	High	Total
Remote	Unburned	41	2	0	43
Sensing	Moderate	8	20	13	41
Data	High	1	28	37	66
	Total	50	50	50	150
	Overall	65%			
	Users	82%	40%	74%	
	Producers	95%	49%	56%	

Table 18. Results of all Landsat burn severity remote sensing indices.

dNBR		Reference Data			
		Unburned	Moderate	High	Total
Remote Sensing Data	Unburned	43	2	0	45
	Moderate	6	19	13	38
	High	1	29	37	67
	Total	50	50	50	150
	Overall	66%			
	Users	86%	38%	74%	
	Producers	96%	50%	55%	

NDSWIR		Reference Data			
		Unburned	Moderate	High	Total
Remote Sensing Data	Unburned	37	4	0	41
	Moderate	12	17	17	46
	High	1	29	33	63
	Total	50	50	50	150
	Overall	58%			
	Users	74%	34%	66%	
	Producers	90%	37%	52%	

MSAVI		Reference Data			
		Unburned	Moderate	High	Total
Remote Sensing Data	Unburned	45	3	0	48
	Moderate	4	21	17	42
	High	1	26	33	60
	Total	50	50	50	150
	Overall	67%			
	Users	90%	42%	66%	
	Producers	94%	50%	55%	

RdNBR		Reference Data			
		Unburned	Moderate	High	Total
Remote Sensing Data	Unburned	43	1	0	44
	Moderate	6	28	12	46
	High	1	21	38	60
	Total	50	50	50	150
	Overall	73%			
	Users	86%	56%	76%	
	Producers	98%	61%	63%	

SAVI		Reference Data			
		Unburned	Moderate	High	Total
Remote	Unburned	45	3	0	48
Sensing	Moderate	4	22	16	42
Data	High	1	25	34	60
	Total	50	50	50	150
	Overall	66%			
	Users	90%	44%	68%	
	Producers	94%	52%	57%	

Appendix II: Other Remote Sensing Indices Applied

Two other remote sensing indices using the modified NDVI index were performed to test their accuracy and compare their results with other indices. Results presented previously were limited to the best indices. Because the SWIR band is useful for fire detection, it was incorporated into the NDVI index by replacing the NIR band. The post-fire SPOT image was used to create the post modified NDVI (pModNDVI) (Table 19). The differenced modified NDVI (dModNDVI) was created using both the pre-fire and post-fire SPOT images (Table 19).

The dModNDVI and rModNDVI (presented previously) had the same overall accuracy for burn severity results (Tables 20 and 14, respectively), but the dModNDVI had slightly lower overall accuracy for the burned versus unburned results (Table 21). Though the pModNDVI overall accuracy results for burned versus unburned (Table 21) were similar to results already presented, its burn severity results were very poor.

Table 19. Other remote sensing indices to detect burn severity.

Remote Sensing Index	Algorithm	Sensor
pModNDVI	$\frac{SWIR - Red}{SWIR + Red}$	SPOT: Red = band 2 SWIR = band 4
dModNDVI	Pre-fire ModNDVI – Post-fire ModNDVI	

Table 20. 'Burn severity' accuracies and kappa statistics for other remote sensing indices using SPOT 5 imagery.

Accuracy Type	pModNDVI	dModNDVI
Overall Accuracy	53%	67%
Producer's Unburned	100%	98%
Users Unburned	32%	80%
Producer's Moderate	35%	53%
Users Moderate	42%	42%
Producer's High	58%	58%
User's High	84%	80%
KHAT	0.3	0.5100
Variance	0.004045	0.0033
Z Stat	4.716899	8.8441

Table 21. 'Burned versus unburned' accuracies and kappa statistics for other remote sensing indices using SPOT 5 and imagery.

Accuracy Type	pModNDVI	dModNDVI
Overall Accuracy	84%	93%
Producer's Unburned	100%	98%
Users Unburned	34%	80%
Producer's Burned	82%	91%
Users Burned	100%	99%
KHAT	0.435897	0.8272
Variance	0.007515	0.0024
Z Stat	5.02837	16.6233

Appendix III: Details of the Landsat and SPOT sensors

Table 22. Comparison of Landsat 7 and SPOT 5 sensor characteristics (Lillesand et al., 2004).

	Landsat 7 ETM+	SPOT 5
Dates	August 27, 2005 September 28, 2005	July 4, 2005 October 24, 2005
Spatial Resolution	30 mpp-- multispectral 60 mpp-- Thermal 15 mpp-- Panchromatic	10 mpp-- multispectral 20 mpp-- SWIR 2.5 mpp-- Panchromatic
Bands and Spectral Resolution (μm)	1 0.45 - 0.52 (Blue) 2 0.52 – 0.60 (Green) 3 0.63 – 0.69 (Red) 4 0.76 – 0.90 (NIR) 5 1.55 – 1.75 (SWIR) 6 10.4 – 12.5 (Thermal) 7 2.08 – 2.35 (MIR) 8 0.52 – 0.90 (Panchromatic)	1 0.50 – 0.59 (Green) 2 0.61 – 0.68 (Red) 3 0.78 – 0.89 (NIR) 4 1.58 – 1.75 (SWIR) 5 0.48 – 0.71 (Panchromatic)
Cost/100 km^2	$275 (gap-filled)	$406
Operational Altitude (km)	705	832
Swath Width (km)	185	60-80
Phase Orbit	16 Days	26 Days
Launch	April 15, 1999	May 3, 2002
Image Area (km^2)	31,450	3600

Appendix IV: Assessment of Hypothesis #2: Can burn severity be predicted with fuel load?

It is hypothesized that fuel load can be used to reliably predict burn severity, and thus pre-burn conditions can be derived (post-burn) using remote sensing derived burn severity. Only moderate and high burn severity data (n = 193 plots) could be used in this analysis because the unburned data locations were biased. Except for two plots within the burn, the unburned plots were chosen and intentionally NOT burned. Taking into consideration georegistration errors, two unburned plot samples are not enough to include in the data analysis. Therefore, the question became: can moderate and high burn severity be predicted with fuel load?

A Spearman correlation method was used (because there is a non-parametric distribution) to assess the correlation between fuel load ocular estimates and remote sensing index burn severity values. Fuel load categories were 1, 2, and 3, and the burn severity category was continuous. The Landsat relative dNBR values are significantly correlated with fuel load ($P < 0.001$) but moderately ($rho = 0.292$). SPOT SAVI values are also significantly correlated with fuel load ($P < 0.0001$), however, these values do not predict fuel load well ($rho = -0.362$).

In addition, a Spearman correlation method was used (because there is a non-parametric distribution) to assess the correlation between fuel load ocular estimates and remote sensing index burn severity values that were put into ordinal categories. Index values were placed into ordinal categories (unburned, moderate severity, and high severity) the same as described above. Fuel load categories were 1, 2, and 3, and burn severity categories were 2 and 3. Burn severity is not significantly correlated with fuel load ($P = 0.5273$, $rho = 0.046$) using the SPOT SAVI data; and fuel load

does not predict burn severity significantly nor well (P = 0.2049, rho = 0.092) using the Landsat relative dNBR data.

These results conclude that pre-burn conditions cannot be derived post burn using remote sensing data. This may be due to a combination of factors such as timing of field data collection, timing of imagery, span of time between pre-and post-fire images and georegistration errors. Additionally, SPOT lacks the spectral resolution for adequate burn severity classification and although Landsat demonstrated a greater sensitivity of burn severity, fuel load still did not have a significant effect, perhaps due to Landsat's spatial resolution. Higher-than-normal amounts of pre-fire fuel load and high winds during the fire contributed to most of the study area having high burn severity. Though the nature of fire is sporadic and pre-fire fuel loads cannot be controlled, a more orthogonal design may better detect the relationship between fuel load and burn severity. Also, before the fire, fuel load was fairly homogenous across the study area. This study could be improved by having more sample plots in the unburned area and not so heavily weighted with high burn severity plots.

Appendix V: Comparison of Field Methods

INTRODUCTION

Collecting field data from an entire study site is often not practical, thus sampling is often performed. Sampling takes measurements on small plots that are representative of the larger study site. Most sampling methods are quantitative and can include measures of frequency, biomass, and/or cover. The latter measure, canopy cover is a measure of percentage of all ground cover such as vegetation, litter, and bareground. Cover is a measure of abundance that is not biased by the size and distribution of individuals (Floyd and Anderson, 1987; Floyd and Anderson, 1982). A challenging aspect of cover measurements is relating percent canopy cover to remote sensing data and measurements. Cover can be measured in many ways in the field; common methods include ocular estimate (Peterson, 2005), point (Friedel and Chewings, 1988), line (Rahman and Gamon, 2004), or quadrat (Hanley, 1978), surveys. Ocular estimation is most often represented as the percentage of total cover (Carlsson et al., 2005) within a plot as opposed to point, line, and quadrat methods which are direct measurements (Hanley, 1978).

Several studies have compared cover methods in grasslands and rangelands to assess the agreement between them (Hanley, 1978; Stohlgren et al., 1998; Carlsson, 2005). Within sagebrush (*Artemisia* ssp.) steppe ecosystems, Hanley (1978) and Floyd and Anderson (1987) concluded that line and point interception are more precise than visual (ocular) estimation. Kinsinger et al. (1960) determined that line interception was most accurate compared with two other canopy coverage techniques. Furthermore, Floyd and Anderson (1982) determined that point and line intercept

methods provided similar results but that the line intercept required 32% more time for the same precision. Their 1987 study compared sampling time and precision between three cover estimate techniques and it revealed that point interception is the most efficient. The point frame technique is a well-accepted, accurate sampling method (Hanley, 1978; Floyd and Anderson, 1982; Floyd and Anderson, 1987; Inouye, 2002). Prior to its design, line interception was one of the most widely used cover methods in shrubby vegetation (Floyd and Anderson, 1982). Created by Floyd and Anderson (1982) in sagebrush steppe ecosystems, the point frame establishes a dot grid overlooking underlying vegetation and bareground.

There are several types of ocular methods; each can be modified based on the users' sampling needs and experimental design. They typically involve a walk-about viewing the vegetation, soil, and other ground cover across the plot then estimating their percentages. The ocular method typically estimates the percent cover of the top canopy layer, as would be viewed by a satellite sensor. Although ocular estimates may provide a less precise and less accurate estimation of cover than other methods, their advantages include the ease and efficiency of data collection and potential for being most applicable to the spatial resolution of remote sensing images (e.g. 10-30 m). Though the ocular method is more time efficient during data collection than the point frame, it requires copious training time in order to minimize user bias. Ocular methods can involve viewing ground cover from different viewpoints such as panoramic and planimetric views. Germino et al., (2001) state that there is poor correlation between panoramic and planimetric landcover methods and that

planimetric methods are better than panoramic methods for landcover studies due to perspective distortions.

We chose the point frame method for comparison to the ocular method because the near nadir view of the vegetation while sampling with a point frame emulates the view of a satellite. The point frame also provides an objective method for comparison to the ocular method. As Floyd and Anderson (1987) pointed out, absolute ground coverages are unknown, therefore it is difficult to compare coverage techniques with absolute certainty.

This study compares a point sighting frame method with an ocular estimation method using two data sets in the same area (+/- 5 m) before and after a prescribed burn (pre-fire n = 44, post-fire n = 42). We aim to determine the correlations between the two methods as well as their applicability for application to 10-30 m remote sensing imagery in rangeland ecosystems. Ground reference data (e.g. cover measurements) are often applied to remote sensing data to 1) aid in the analysis/interpretation of remotely sensed data, 2) calibrate a sensor, and or 3) verify information extracted from remote sensing data (accuracy assessment) (Lillesand, 2004). Although Landsat data have been correlated to ground data for decades, there are few studies that relate precise ground truth data with remote sensing data. While many remote sensing studies use ground-truth data, no well accepted and published guide is available detailing how to routinely collect vegetation cover in rangeland environments to relate to remote sensing imagery. We compared the results of these two cover methods in order to determine which one would be favorable in future rangeland applications. It was hypothesized that the point frame method would be

more accurate in estimating ground cover based on the discussion above. The proportion of intercepted points averages the cover of that cover type and thus provide a better measurement for remote sensing accuracy assessment. There is flexibility in adjusting both point frame and ocular plot sizes to the scale of the imagery, yet the precision of the point frame is higher than that of an ocular estimate of ground cover.

METHODS

The study area is the Hitching Post pasture, a 3.24 km^2 fenced parcel within the U.S. Sheep Experiment Station (USSES) located in Clark County, Idaho (Fig. 1). The pasture is a sagebrush steppe ecosystem characterized by extreme seasonal variability and a co-dominance of *Artemisia* with several grass species (West and Young, 2000). This semiarid area has an elevation of 1463 m, an average annual precipitation of 250-530 mm, and average annual temperatures of 5°-6°C, with a 70 to 90 day frost-free season. The majority of the study area has gradual slopes (0%-1.5%). Soils are mixed, fine-loamy, frigid Calcic Argixerolls derived from residuum, alluvium, or windblown loess (Seefeldt, 2005; Natural Resources Conservation Service, 1995). Cattle and horses have grazed this pasture for the last decade, but it has been rested for the past two and a half years. No fires have occurred in the study area for the past 10 years and most of the area has moderate fuel load (≈ 6722 kg·hectare). The study area was stratified for sampling based on fuel load because vegetation biomass was unaffected by slope, soil type, grazing, or fire history.

The pasture is within a sagebrush steppe ecosystem and has two primary subspecies of sagebrush (*Artemisia* ssp.), mountain big (*A. tridentata* ssp. *vaseyana*)

and threetip sagebrush (*A. tripartita ssp. tripartita*); other shrub species include antelope bitterbrush (*Purshia tridentata*), green rabbitbrush (*Chrysothamnus viscidiflorus)*, and horsebrush (*Tetradymia canescens)*. There are a few small patches of the exotic forbs leafy spurge (*Euphorbia esula*) and spotted knapweed (*Centaurea maculosa*); the exotic annual, cheatgrass (*Bromus tectorum)*, occurred as a small component (<1%) of the overall plant cover. Lupine (*Lupinus argenteus)* is the most plentiful forb in the pasture, ranging in height from 20 cm to 1 m. During field sampling in summer 2005, sparse bareground was observed, and live vegetation cover (sagebrush, forbs, and grass) was high. This study area was chosen because of the opportunity to participate in a prescribed burn (September 23 and 24, 2005), allowing a high degree of control for pre- and post-fire field sampling.

Though there is not a standard point frame plot size, we determined our plot size to be 20 x 40 m according to the smallest satellite imagery pixel size used in a related study (10-20 m resolution, SPOT 5). This plot size directly relates to at least two (ideally eight with precise georegistration) pixels and therefore provides more accurate comparisons between field data and remote sensing data. Vegetation and/or soil in point frames were assigned to six categories: shrub, grass, forb, litter, rock, and bareground. Shrubs, forbs, and grasses were recorded if photosynthetic tissue fell under a point; shrub stem, dead or alive, and downed combustible debris were recorded as litter if it fell under a point; and rock or bareground were recorded if they were under a point. The necessary number of frames per plot were determined using sample effort curves (Fig. 2), sufficient to capture the variability within the cover types in the study area consisted of 15 frames within each plot. The 15 frames

collected within each 20 x 40 m plot used a point frame (0.5 x 1 m with 36 points at 0.1 m intervals) placed ≈1 m aboveground, totaling 540 point observations per plot (Fig. 3). Forty-nine random point frame plots were collected with the following criteria: 1) >20m from all bulldozer-created black-lines (for enclosure of the prescribed burn), and 2) >20m from all roads to mitigate road effects. Before the fire we sampled the 49 random plots, and post-fire we sampled 42 of the same random plots (within +/- 5 m). Plot boundaries were recorded with a Trimble GeoXT GPS receiver (+/- 0.7m @ 95% CI) (Serr, unpublished).

The ocular estimate method used mimics that developed by the ISU GIS TReC (2006) in 1999 and modified by McMahan et al. (2003) for semiarid rangelands in southeastern Idaho. In this method, six cover classes are used to visually assess percent of ground cover by two observers over a 60 m x 60 m plot which ideally covers four Landsat 30 x 30 m pixels or at least two pixels. Each person starts in the plot center and paces 30 m in opposite directions to the plot boundary. After walking the plot circumference, they proceed to walk in a spiral pattern within 3-4 m of the previous track back towards the plot center while observing plot attributes. At the center, each plot attribute is discussed until agreed upon. The six cover classes collected include shrub, grass, forb, litter, bareground, and rock. Categorical groups (Table 2) are used to assess percent cover for each cover class (McMahan et al., 2003). The same 42 random plots (as point frame plots) were navigated to both pre- and post-fire for this method so that cover class correlations could be fairly assessed. Each plot center location was recorded using a Trimble GeoXT GPS receiver (+/- 0.7m @ 95% CI) (Serr, unpublished). Other

attributes of the point frame method (Table 4) are compared with the ocular method attributes.

Polynomial correlation was used to analyze the variability between the ocular and point frame estimates of ground cover. Before remote sensing could be performed, this was the most appropriate statistical technique for preliminary data analysis. Since both variables (point frame estimates and ocular estimates) were response variables and there was no assumption that one would predict the other, correlation was chosen over regression. Significances for ground cover were compared by applying analysis of variance (ANOVA) for each cover category in each data set (pre-fire data set n = 49; post-fire data set n = 42) using SAS (SAS Institute Inc., 2005).

RESULTS

Correlation analyses between the point frame and ocular estimates were performed with the pre-fire and post-fire field collected data sets. Data show that shrub has the best correlation coefficient for both pre-fire and post-fire data sets (Figures 11 and 12). For the pre-fire data, shrub is the only cover that has fair correlation 79%; bareground has the next best correlation, a weak 65%. However, for the post-fire data, shrub, forb, and bareground have strong correlation, 89%, 83%, and 81% respectively. Litter and rock correlations are poor for pre-fire data (38% and 45% respectively), yet post-fire correlations improve to 74% and 53% respectively. Therefore, point frame and ocular estimate correlations improved after the prescribed burn.

DISCUSSIONS AND CONCLUSIONS

The shrub cover had the best correlation between ocular and point frame estimates, likely because of its relatively large size (scale) and thus easy for the human eye to estimate total cover. Our lowest correlations with pre-fire data were with litter and rock, hypothesized to be due to their fine scale and thus difficulty to interpret. All post-fire correlations were higher between field methods, most likely because visually assessing cover on the same plane (i.e. burned landscapes) is easier than assessing cover with multiple canopy levels (i.e. vegetated landscapes).

The shrub cover class has overwhelmingly more height and depth than the other classes. Grass and forbs also have height and depth but they are much shorter and not as broad. Litter, bareground, and rock have relatively little height or depth; these classes are at ground level (except for some litter and shrub stem) and tend to cover a more continuous area than the vegetation classes. These characteristics are pertinent to the perspective of the observer(s).

Because pre-fire vegetation at our study site had a variety of height and depth characteristics, panoramic observations through the ocular method are likely poor estimates. Though our ocular estimates involved walking the plot extensively, we didn't have a completely nadir view upon the ground cover, as the point frame did. Thus the point frame results have better accuracy in the pre-fire estimates. On the other hand, the post-fire ground cover had fewer canopy levels (often just one), with less vegetation and more exposed litter, bareground, and rock. As our post-fire

correlation results show, it was easier to ocularly estimate cover with fewer canopy levels and more continuous cover.

Field methods for determining ground cover must take into account perspective distortions such as line of sight and distance effects (Germino et al., 2001). For example, observations taken only from the plot center are error prone. Thus a nadir view of underlying vegetation is necessary to mitigate these effects. Therefore if ocular methods are used, the viewer must walk the plot in a small-scale, grid-like fashion in order to view in nadir the vegetation across the whole plot. The ocular estimations could be improved by decreasing the grid size and using a complete nadir observation stance. The point frame observations were taken at a small scale (0.5 x 1.0 m) with 15 frame estimates across the plot. More point frames may increase the accuracy and precision through observing more of the plot.

The intention of this project was to correlate two field methods for estimating ground cover in rangelands in order to determine the best method for application with 10-30 m remote sensing data. A method which correlates with remote sensing data will enhance training data and thus provide better accuracy assessments. We show that the point frame may be more accurate for dense vegetation, whereas the ocular method may be more appropriate in single canopy or extremely sparse vegetation. The only exception to this is the shrub category which had high correlation, therefore it may be applicable to estimate its cover alone for application to remote sensing imagery. The point frame method is a practical option because it provides better overall accuracy, no subjectivity/user bias is introduced, and it has good repeatability which is essential in multi-temporal studies. It takes only two to three times more

sampling time (Table 23) than ocular methods, with relatively no training time. Because ocular estimates require less field time for each plot and thus more area can be covered, it is also an attractive option for ground truthing purposes. We've shown that both methods are feasible for ground truthing purposes as long as scale, number of canopy levels, and perspective distortions are taken into consideration so that ground cover units are not compromised. The results of this analysis are the backbone for future correlational studies between cover methods and application to remote sensing data.

REFERENCES

Carlsson, A.L.M., Bergfur, J., and Milberg, P. (2005). Comparison of data from two vegetation monitoring methods in semi-natural grasslands. *Environmental Monitoring and Assessment*, 100, 235-248

Floyd, D. and J. Anderson. (1982). A New Point Frame for Estimating Cover of Vegetation. *Vegetatio* 50: 185-186.

Floyd, D. and J. Anderson. (1987). A Comparison of Three Methods for Estimating Plant Cover. *Journal of Ecology* 75: 221-228.

Friedel, M.H. and Chewings, V.H. (1988). Comparison of crown cover estimates for woody vegetation in arid rangelands. *Austral Ecology*, 13, 463-468

Germino, M.J., Reiners, W.A., Blasko, B.J., McLeod, D., and Bastian, C.T. (2001). Estimating Visual Properties of Rocky Mountain Landscapes Using GIS. *Landscape and Urban Planning* 53: 71-83.

GIS TReC. (2006). GIS Training and Research Center. URL: http://giscenter.isu.edu/software/index.htm Last accessed: October 16, 2006.

Hanley, T.A. (1978). A Comparison of the Line-Interception and Quadrat Estimation Methods of Determining Shrub Canopy Coverage. *Journal of Range Management* 31:60-62.

Inouye, R. (2002). Sampling Effort and Vegetative Cover Estimates in Sagebrush Steppe. *Western North American Naturalist* 62(3): 360-364.

Kinsinger, F.E., Eckert, R.E., and Currie, P.O. (1960). A comparison of the line-interception, variable-plot, and loop methods as used to measure shrub crown cover. *Journal of Range Management*, 13, 17-21

Lillesand, T.M., Kiefer, R.W., and Chipman, J.W. (2004). *Remote Sensing and Image Interpretation.* (pp. 1-500). New York: Wiley

McMahan, J.B., Narsavage, D., and Weber, K.T. (2003). "The Pole Cam": Corroborating field estimations with High Spatial Resolution Imagery. http://giscenter.isu.edu/research/techpg/nasa_wildfire/Final_Report/Documents/Chapter3.pdf.

Natural Resources Conservation Service (NRCS). (1995). Soil investigation of Agriculture Research Service, United States Sheep Experiment Station headquarters range, US Department of Agriculture. (pp. 133). Rexburg, ID: NRCS

Peterson, E.B. (2005). Estimating cover of an invasive grass (Bromus tectorum)

using tobit regression and phenology derived from two dates of Landsat ETM+ data. International Journal of Remote Sensing 26, 2491-2507.

Rahman, A. and Gamon, J. (2004). Detecting biophysical properties of a semi-arid grassland and distinguishing burned from unburned areas with hyperspectral reflectance *Journal of Arid Environments,* 58, 597-610

SAS Institute Inc., (2005). Cary, NC, USA

Seefeldt, S.S. (2005). Consequences of selecting rambouilllet ewes for mountain big sagebrush (Artemisia tridentata ssp. vaseyana) dietary preference. *Rangeland Ecology and Management,* 58, 380-384

Stohlgren, T.J., Bull, K.A., and Otsuki, Y. (1998). Comparison of rangeland vegetation sampling techniques in the central grasslands. *Journal of Range Management*, 51, 164-172

West N.E. and Young, J.A. (2000). Intermountain Valleys and Lower Mountain Slopes. In M.G. Barbour and W.D. Billings (Ed.), *North American Terrestrial Vegetation* (pp. 255-284). Cambridge, UK: Cambridge University Press

TABLES AND FIGURES

Table 23. Attributes of the ocular and point frame vegetation cover field methods.

	Ocular	Point Frame
Time per plot	15-20 minutes	30-40 minutes
Accuracy	Low	0.5 x 1.0 m
Precision (repeatability)	Poor	High
Scale (extent)	60 m x 60 m	20 m x 40 m

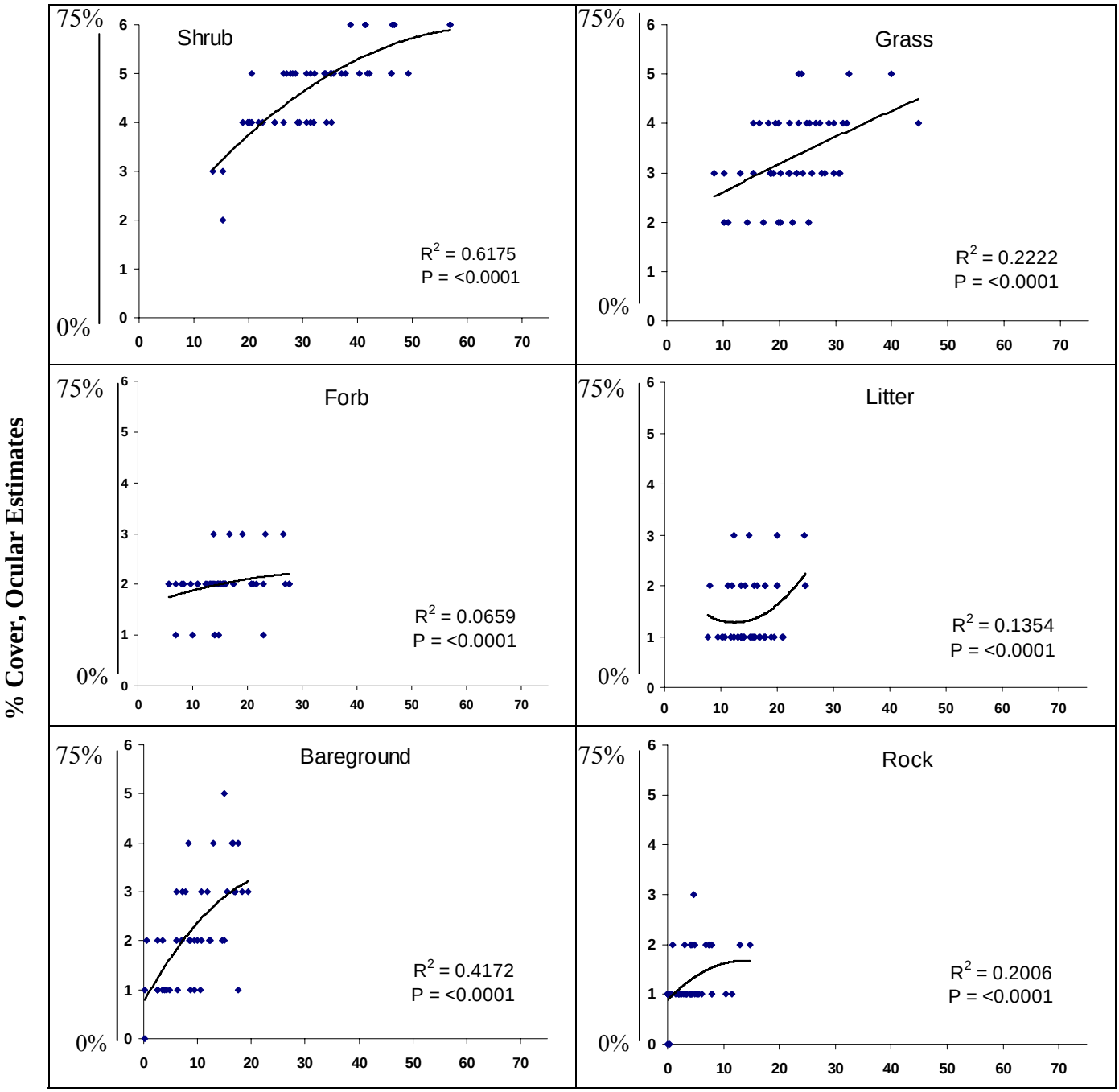

Figure 11. Using the pre-fire data set, point frame estimates are fairly correlated with ocular estimates (n = 49) in the same area for shrub and bareground.

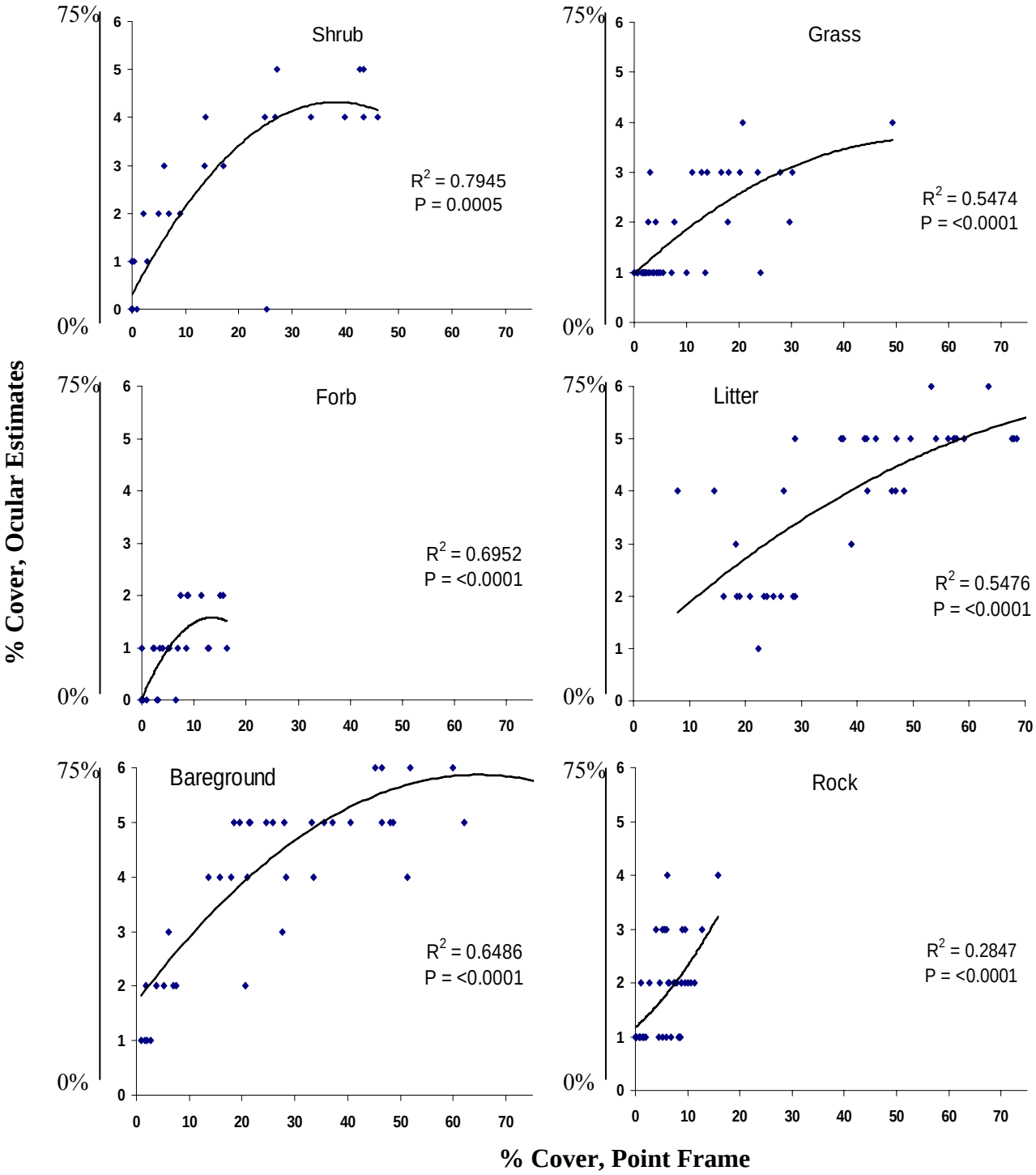

Figure 12. Using the post-fire data set, the best correlation between point frame estimates and ocular estimates are for shrub (best overall correlation) and forb.

Additional Results to be contemplated:

Table 24. Maximum percent of cover within each cover class using ocular and point frame data collected before the fire.

	Ocular Estimates						Point Frame Estimates					
	Shrub	Grass	Forb	Litter	Bare-ground	Rock	Shrub	Grass	Forb	Litter	Bare-ground	Rock
0%												
1-5%				65%	31%	71%						57%
6-15%			80%						53%	59%	49%	
16-25%		43%						53%				
26-35%							41%					
36-50%	45%											
51-75%												
> 75%												

Table 25. Maximum percent of cover within each cover class using ocular and point frame pre-fire data collected after the fire.

	Ocular Estimates						Point Frame Estimates					
	Shrub	Grass	Forb	Litter	Bare-ground	Rock	Shrub	Grass	Forb	Litter	Bare-ground	Rock
0%	48%		57%				55%		50%			
1-5%		60%				45%		43%				
6-15%												55%
16-25%											21%	
26-35%												
36-50%				48%	36%					31%		
51-75%										31%		
> 75%												